

125 GEV HIGGS BOSON MASS FROM  
5D GAUGE-HIGGS UNIFICATION

by

JASON CARL CARSON

NOBUCHIKA OKADA, COMMITTEE CHAIR

BENJAMIN C. HARMS

SANJOY K. SARKER

PAOLO RUMERIO

KAUSTUBH AGASHE

A DISSERTATION

Submitted in partial fulfillment of the requirements  
for the degree of Doctor of Philosophy  
in the Department of Physics and Astronomy  
in the Graduate School of  
The University of Alabama

TUSCALOOSA, ALABAMA

2015

Copyright Jason Carl Carson 2015  
ALL RIGHTS RESERVED

## ABSTRACT

In the context of a simple gauge-Higgs unification (GHU) scenario based on the gauge group  $SU(3)\times U(1)'$  in a 5-dimensional flat space-time, we investigate a possibility to reproduce the observed Higgs boson mass of around 125 GeV. We introduce bulk fermion multiplets with a bulk mass and a (half) periodic boundary condition. In our analysis, we adopt a low energy effective theoretical approach of the GHU scenario, where the running Higgs quartic coupling is required to vanish at the compactification scale. Under this “gauge-Higgs condition,” we investigate the renormalization group evolution of the Higgs quartic coupling and find a relation between the bulk mass and the compactification scale so as to reproduce the 125 GeV Higgs boson mass. Through quantum corrections at the one-loop level, the bulk fermions contribute to the Higgs boson production and decay processes and deviate the Higgs boson signal strengths at the Large Hadron Collider (LHC) experiments from the Standard Model (SM) predictions. Employing the current experimental data which show the the Higgs boson signal strengths for a variety of Higgs decay modes are consistent with the SM predictions, we obtain lower mass bounds on the lightest mode of the bulk fermions.

## LIST OF ABBREVIATIONS AND SYMBOLS

4D	Four-dimensional
5D	Five-dimensional
$\epsilon_{i,j,k}$	Levi-Civita Tensor
$f_{abc}$	$SU(3)$ structure constants
GHU	Gauge Higgs unification
$M_P$	Planck Mass
$RG$	Renormalization group
$\sigma^i$	Pauli Matrices
SM	Standard Model
$T^a$	Gell-Mann Matrices
$VEV$	Vacuum expectation value

## **ACKNOWLEDGEMENTS**

I would first like to thank my parents Donna G. Anderson and Carl F. Carson. Their love and support have allowed me to accomplish so much. I would also like to thank my stepparents Eli Anderson and Kim Carson who loved and treated me as if I was their own child. My grandmother Gail Albright was also instrumental in my success with her love and support along with my grandfather Don Albright whom did not live to see this day. These individuals have made so many sacrifices that have allowed me to be where I am today and for that I am ever grateful. My siblings (Jeremy Carson and Jessica Milum) also deserve thanks for their support and love. Finally I have several friends I would like to thank for helping keep me sane during this venture.

## CONTENTS

<b>ABSTRACT</b> . . . . .	ii
<b>LIST OF ABBREVIATIONS AND SYMBOLS</b> . . . . .	iii
<b>ACKNOWLEDGEMENTS</b> . . . . .	iv
<b>LIST OF TABLES</b> . . . . .	vii
<b>LIST OF FIGURES</b> . . . . .	ix
<b>1 INTRODUCTION</b>	<b>1</b>
<b>2 INTRODUCTION TO THE STANDARD MODEL</b>	<b>4</b>
2.1 Standard Model Gauge Groups . . . . .	4
2.2 Particle Content of the Standard Model . . . . .	8
2.3 Electroweak Symmetry Breaking . . . . .	8
2.4 Hierarchy Problem . . . . .	11
<b>3 <math>SU(3) \times U(1)'</math> GHU MODEL</b>	<b>16</b>
3.1 Kaluza Klein Compactification . . . . .	16
3.2 $SU(3)$ Toy Model . . . . .	17
3.3 Correct Weinberg Angle at Tree Level . . . . .	24
3.4 Correct Fermion Mass Spectrum . . . . .	25
<b>4 GAUGE HIGGS CONDITION</b>	<b>29</b>
4.1 Effective Potential and Higgs Mass in $SU(3)$ Toy Model . . . . .	29
4.2 Deriving the Gauge-Higgs Condition . . . . .	31
4.3 Higgs Mass from the Gauge-Higgs Condition . . . . .	32
<b>5 HIGGS BOSON MASS WITH THE GAUGE-HIGGS CONDITION</b>	<b>37</b>
<b>6 HIGGS BOSON PRODUCTION AND DECAY IN GHU MODEL</b>	<b>47</b>

6.1	Bulk Fermion Contributions to the Gluon Fusion Channel . . . . .	47
6.2	Bulk fermion contributions to $h \rightarrow \gamma\gamma$ . . . . .	51
6.3	Bulk colored fermion contributions to $gg \rightarrow h \rightarrow \gamma\gamma$ . . . . .	54
<b>7</b>	<b>CONCLUSIONS</b>	<b>58</b>
	<b>REFERENCES</b>	<b>61</b>

## LIST OF TABLES

2.1	SM gauge symmetries and their corresponding gauge fields. . . . .	7
2.2	Particle content of the standard model . . . . .	8
6.1	The lower bound on the lightest bulk fermion masses and the compactification scales from the ATLAS and CMS combined analysis, $0.88 \leq R_{gg} \leq 1.2$ , for the cases with the color-triplet, <b>6</b> or <b>10</b> -plet bulk fermion. Here, the initials, “BC”, “P” and “HP” stand for “boundary condition”, “periodic” and “half-periodic”, respectively. We have also shown in the last row the lower bound on the compactification scale when only the top quark KK modes is taken into account. . . . .	51
6.2	The lower bound on the lightest bulk fermion masses and the compactification scales from the ATLAS and CMS combined analysis, $0.98 \leq \mu^{\gamma\gamma} \simeq R_{\gamma\gamma} \leq 1.36$ , for the cases with the color-singlet, <b>6</b> and <b>10</b> -plet bulk fermions. . . .	54
6.3	The lower bound on the lightest bulk colored fermion masses and the compactification scales from the ATLAS and CMS combined analysis, $0.98 \leq \mu^{\gamma\gamma} \leq 1.36$ . We have obtained the lower bound only for the <b>10</b> -plet bulk fermions.	54



## LIST OF FIGURES

2.1	Feynman diagram of top loop correction to Higgs boson propagator . . . . .	13
2.2	Higgs Quartic coupling running at next-to-next to leading order propogator. This figure is from Ref. [1]. . . . .	14
3.1	An illustration of an $S^1/Z_2$ orbifold. . . . .	19
4.1	Tadpoles diagrams contributing to the effective potential . . . . .	30
4.2	The RG evolution of the Higgs quartic coupling in the SM for the input of the Higgs boson pole mass $m_H = 125.09$ GeV. . . . .	33
5.1	The RG evolutions of the Higgs quartic coupling, which can reproduce the Higgs boson pole mass $m_H = 125.09$ GeV. The solid line denotes the running Higgs quartic coupling in the SM. The dashed and dotted lines correspond, respectively, to the <b>6</b> -plets for $N_f = 2$ , $N_c = 1$ , $Q = 2/3$ and $(M_{KK}, m_0) = (12.7, 1.5)$ TeV, and the <b>6</b> -plet for $N_f = 2$ , $N_c = 3$ , $Q = 4/3$ and $(M_{KK}, m_0) = (5.65, 1.5)$ TeV. . . . .	41
5.2	The RG evolutions of the SM SU(2) gauge coupling (solid line) and Yukawa couplings $ Y_S $ (dashed line) and $ Y_D $ (dotted line) for the case with $N_f = 1$ pair of <b>6</b> -plet, color singlet bulk fermions. We can see that the boundary condition from the unification among the gauge and Yukawa couplings, $ Y_S  =  Y_D  = g_2$ , is satisfied at $M_{KK} = 12.7$ TeV. . . . .	42
5.3	The relation between $M_{KK}$ and $m_0$ to reproduce the Higgs boson pole mass $m_H = 125.09$ GeV. The top panel shows the results for the color singlet, <b>6</b> -plet bulk fermions with $N_f = 1$ (solid line) and $N_f = 2$ (dashed line). Here we have taken $Q = 2/3$ . The bottom panel shows the results for the color triplet, <b>6</b> -plet bulk fermions with $N_f = 1$ (solid line) and $N_f = 2$ (dashed line). For the color triplet case, we have taken $Q = 4/3$ . . . . .	43
5.4	The relation between $M_{KK}$ and $m_0$ to reproduce the Higgs boson pole mass $m_H = 125.09$ GeV for various U(1)' charges. The solid, dashed and dotted lines corresponds to the results for $Q = 0, 2$ and $-2$ , respectively. . . . .	44
5.5	The relation between $M_{KK}$ and $m_0$ to reproduce the Higgs boson pole mass of $m_H = 125.09$ GeV. The solid and dashed lines denote the results for the color singlet, <b>10</b> -plet bulk fermions with $N_f = 1$ and $N_f = 2$ , respectively. Here we have taken $Q = 1$ . The dotted and dash-dotted lines represent the results for the color triplet, <b>10</b> -plet bulk fermions with $N_f = 1$ and $N_f = 2$ ( $N_f^{\text{HP}} = 1$ ), respectively. We have taken $Q = 5/3$ for the <b>10</b> -plets. . . . .	46

6.1	The ratio of the Higgs production cross section in our model to the SM one as a function of the lightest bulk fermion mass $m_0$ . The top panel shows the results for the <b>6</b> -plet case corresponding to the bottom panel of Fig. 5.3. The results for the <b>10</b> -plet case, corresponding to the dotted and dash-dotted lines in Fig. 5.5, are depicted in the right panel. Here we have considered the periodic boundary condition for the dotted line in Fig. 5.5, while the half-periodic boundary condition for the dash-dotted line Fig. 5.5. The dotted and dash-dotted lines represent the results for the periodic and half-periodic <b>10</b> -plet fermions, respectively. . . . .	50
6.2	The signal strength for the Higgs diphoton decay mode in our model as a function of the lightest bulk fermion mass $m_0$ . The top panel shows the results for the <b>6</b> -plet case corresponding to the top panel of Fig. 5.3. The results for the <b>10</b> -plet case, which correspond to the solid and dashed lines in Fig. 5.5, are depicted in the bottom panel. . . . .	55
6.3	The signal strength as a function of the lightest bulk fermion mass $m_0$ . The top panel shows the results for the <b>6</b> -plet case corresponding to the top panel of Fig. 5.3. The results for the <b>10</b> -plet case, corresponding to the dotted and dash-dotted lines in Fig. 5.5, are depicted in the bottom panel. Here we have considered the periodic boundary condition for the dotted line in Fig. 5.5, while the half-periodic boundary condition for the dash-dotted line Fig. 5.5. The dotted and dash-dotted lines represent the results for the periodic and half-periodic <b>10</b> -plet fermions, respectively. . . . .	57

## 1 INTRODUCTION

The discovery of the Standard Model (SM) Higgs boson by ATLAS [2] and CMS [3] collaborations at the Large Hadron Collider (LHC) is a milestone in the history of particle physics, and the experimental confirmation of the SM Higgs boson properties has just begun. A recent combined analysis by the ATLAS and the CMS [4] has determined the Higgs boson mass very precisely as  $m_H = 125.09 \pm 0.21(\text{stat.}) \pm 0.11(\text{syst.})$  GeV. It has been shown that by combined ATLAS and CMS measurements [5] that the Higgs boson production and decay rates are consistent with the SM predictions. Although the current LHC data include less indications for the direct productions of new particles, the Higgs boson can be a portal to reveal new physics beyond the SM through more precise measurements of the Higgs boson properties and their possible deviations from the SM predictions.

Despite its success the SM still doesn't address several issues. An interesting issue within the SM is the gauge hierarchy problem. This issue addresses the fact that the Higgs boson mass isn't stable against quantum corrections. In order to provide a solution to this problem the standard model requires an unnatural amount of fine tuning between the bare Higgs mass and its radiative corrections. Even if we assume the standard model simply requires such a level of fine tuning we are still left with the fact that the Higgs quartic coupling goes negative at high energies.

In this dissertation we propose a solution to these issues in terms of the gauge-Higgs unification scenario (GHU). In the GHU scenario, the SM Higgs doublet is identified as an extra spatial component of the gauge field in higher dimensional theory, and the higher-dimensional gauge invariance forbids the quadratic divergences in the self-energy corrections of the Higgs doublet in the SM as an effective 4-dimensional theory of the GHU scenario [6]. As a result, the gauge hierarchy problem can be solved. In this dissertation, we focus on a simple GHU scenario in the flat 5-dimensional space-time and assume that the SM is realized as a low energy effective theory of the scenario. It has been pointed out [7] that in this case the running SM Higgs quartic coupling ( $\lambda_H(\mu)$ ) must satisfy a special

boundary condition (gauge-Higgs condition), namely,  $\lambda_H(M_{\text{KK}}) = 0$ , where the  $M_{\text{KK}}$  is the compactification scale of the 5th dimension (Kaluza-Klein mass). In [7] this condition is derived as a renormalization condition for the effective Higgs quartic coupling by using an explicit formula of the effective Higgs potential calculated in the GHU scenario. Since the SM Higgs doublet field is provided as the 5th component of the 5-dimensional gauge field, there is no Higgs potential at tree level in the GHU scenario. The Higgs potential is radiatively generated at low energies with the breaking of the original gauge symmetry down to the SM gauge group by a certain boundary condition under a 5th-dimensional coordinate transformation. Therefore, in the effective theoretical point of view, we expect that once the original gauge symmetry gets restored at some high energy, the Higgs potential must vanish. This is nothing but the gauge-Higgs condition. Note that the gauge-Higgs condition leads to a new interpretation for the electroweak vacuum instability problem in the SM, that is, the energy at which  $\lambda_H(\mu) = 0$  is nothing but the compactification scale and the 5-dimensional GHU scenario takes place there.

The gauge-Higgs condition is a powerful tool to calculate the Higgs boson mass irrespectively to the details of GHU models. The Higgs boson mass is easily obtained by solving the renormalization group (RG) equation of the Higgs quartic coupling by imposing the gauge-Higgs condition at a given compactification scale, when the particle contents and the mass spectrum of the low energy effective theory are defined below the compactification scale.

Since the Higgs self-energy induced through the Kaluza-Klein (KK) modes of the SM particles (plus some extra matters in the bulk) is proportional to  $M_{\text{KK}}^2$ ,  $M_{\text{KK}} = \mathcal{O}(1 \text{ TeV})$  is desired to solve the gauge hierarchy problem. With only the SM particle contents, the GHU scenario with the TeV compactification scale predicts the Higgs boson mass to be too small,  $m_H < 100 \text{ GeV}$ . In order to realize the 125 GeV mass, we need to introduce extra fermions in the bulk. In other words, the observed Higgs boson mass implies the existence of exotic fermions in the context of the GHU scenario. In a simple GHU model based on the  $\text{SU}(3) \times \text{U}(1)'$  gauge group, the Higgs boson mass was calculated in the presence of some bulk fermion multiplets such as **10** and **15** representations under the  $\text{SU}(3)$  [8, 9]. It has been shown that the 125 GeV Higgs boson mass can be realized for the TeV compactification scale. The contributions of the bulk fermions to the Higgs boson production and decay processes

have also been investigated in [8, 9], and the bounds on the exotic fermion masses have been obtained from the current LHC data.

The purpose of this dissertation is to perform detailed analysis for the GHU model in [8, 9] and obtain a more accurate bulk fermion mass spectrum to reproduce the 125 GeV Higgs boson mass. In [8, 9], the Higgs boson mass is calculated by solving the RG equation of the Higgs quartic coupling at the leading-log approximation, and no runnings of the gauge couplings and Yukawa couplings have been taken into account. Although this analysis would be good enough to estimate the order of the exotic fermion masses, the resultant mass spectrum is not accurate enough to discuss the experimental search for the exotic fermions, since the running gauge and Yukawa couplings are expected to be changing a lot in the presence of such a higher-order representation fermions. We will find that our analysis results in the bulk fermion mass spectrum to be very different from the one previously obtained in the rough estimate. This dissertation is organized as follows. In chapter 2 we review the standard model. We will discuss the hierarchy problem and present possible solutions. Chapter 3 will then introduce the  $SU(3) \times U(1)'$  gauge Higgs unification model used in this analysis and some basics of physics in extra dimensions. The gauge-Higgs condition is introduced in chapter 4. In chapter 5 the RG analysis of these new exotic particles needed to solve the gauge hierarchy problem and produce a realistic Higgs mass is done. A realistic mass spectrum of these exotic particles are found. Chapter 6 we examine the effects of these exotic particles on Higgs boson decay and production at the LHC through quantum corrections. Finally Chapter 7 will end the thesis with a conclusion and the findings of this analysis.

## 2 INTRODUCTION TO THE STANDARD MODEL

The SM is a  $SU(3) \times SU(2) \times U(1)$  gauge theory [10, 11, 12]. The gauge symmetries of the SM are continuous and described by Lie groups and their corresponding Lie algebra. It is these gauge symmetries that will bring rise to the gauge boson and fermion interactions of the standard model. In the standard model the  $SU(3)$  gauge symmetry is responsible for the strong force while the  $SU(2) \times U(1)$  gauge symmetry defines the electroweak symmetry. Mass terms are not allowed for these gauge fields due to these gauge symmetries. The  $SU(2) \times U(1)$  symmetry is spontaneously broken by the VEV of a complex scalar  $SU(2)$  doublet. The mechanism for the spontaneous symmetry breaking is known as the Higgs mechanism and will be responsible for the W and Z boson masses along with the fermion masses of the SM [13, 14]. After this symmetry breaking a residual  $U(1)$  electromagnetic symmetry is left.

The SM has achieved great success but can not be a complete theory. This comes from the fact that there many issues that are not explained within the SM. An example is the fact that there is no dark matter candidate in the SM. The case of interest in this thesis and the main reason of this work is the hierarchy problem. The hierarchy problem involves the questions of why the Higgs mass is so small compared to the cutoff scale of the theory. This is often referred to as the "gauge hierarchy problem".

### 2.1 Standard Model Gauge Groups

The SM is created by finding a Lagrangian invariant under an  $SU(3) \times SU(2) \times U(1)_Y$  gauge symmetries. The simplest gauge symmetry of the SM is  $U(1)_Y$  hypercharge symmetry.  $U(1)_Y$  is simple since it only can have one-dimensional irreducible representations and is abelian. By saying it is Abelian it is implied that the order of the successive gauge transformations don't matter. The  $U(1)_Y$  symmetry is given by

$$U_{U_1}(x) = e^{ig_1 Y \Lambda(x)} \tag{2.1}$$

where  $Y$  is defined as the charge of the symmetry and  $g_1$  is the gauge coupling of the symmetry.

To construct a Lagrangian invariant under  $U(1)_Y$  we first start by introducing a  $U(1)_Y$  gauge field. The transformation of this gauge field under  $U(1)$  takes the form

$$B_\mu(x) \rightarrow B'(x) = UB_\mu(x)U^\dagger = B_\mu + \frac{1}{g_1}\partial_\mu\Lambda(x). \quad (2.2)$$

Now in order to allow for fermions interactive with this gauge field we introduce a fermion field with the following transformation under the  $U(1)_Y$  gauge symmetry:

$$\Psi(x) \rightarrow \Psi' = e^{-ig_1Y\Lambda(x)}. \quad (2.3)$$

The final element needed to create this  $U(1)_Y$  invariant Lagrangian is the covariant derivative defined as

$$D_\mu = \partial_\mu + ig_1YB_\mu. \quad (2.4)$$

The covariant derivative is designed this way such that the covariant derivative of a field follows the same transformation rule as the field itself does. A Lagrangian consisting of a single fermion and a  $U(1)$  gauge field invariant under a  $U(1)_Y$  gauge symmetry can be written as follows

$$\mathcal{L} = -\frac{1}{4}B^{\mu\nu}B_{\mu\nu} + i\bar{\Psi}\gamma_\mu D^\mu\Psi \quad (2.5)$$

where  $B_{\mu\nu}$  is the field strength tensor and in the case of  $U(1)_Y$  and is given by

$$B_{\mu\nu} = \partial_\mu B_\nu - \partial_\nu B_\mu. \quad (2.6)$$

$SU(2)$  and  $SU(3)$  are slightly more complex since they are non-abelian. Being non-abelian implies that order matters when taking successive gauge transformations. A  $SU(2)$  gauge transformation can be written as

$$U = e^{ig_2\theta(x)} = e^{ig_2J_R^i w^i(x)} \quad (2.7)$$

where  $J_R^i$  are generators of the group in some representation R,  $g_2$  is the gauge coupling and the repeated indices  $i$  implies a sum over  $i = 1$  to  $i = 3$ . The structure of this gauge group is determined by the Lie algebra of its generators:

$$[J_i, J_j] = i\epsilon_{ijk}J_k, \quad (2.8)$$

where  $\epsilon$  is the 3D Levi-Civita tensor. The fundamental representation of  $SU(2)$ , which is the one we will be interested in, is given by  $J_i = \frac{1}{2}\sigma_i$  where  $i$  runs from one to three and  $\sigma_i$  are the Pauli matrices. Higher dimensional representations can be found by choosing matrices that obey this Lie algebra.

The  $SU(3)$  symmetry is similar to  $SU(2)$  since they both are non-abelian. A  $SU(3)$  symmetry can be written as

$$U = e^{ig_2\eta(x)} = e^{ig_3T_R^a w^a(x)} \quad (2.9)$$

where  $g_3$  is the  $SU(3)$  gauge coupling and  $T_R^a$  are generators in some representation R. The structure of this gauge group is determined by the generators which is defined by the Lie algebra:

$$[T_a, T_b] = if_{abc}T_c, \quad (2.10)$$

where  $f_{abc}$  are the structure constants of  $SU(3)$  which can be found (put in reference). Again we will be interested in the fundamental representation of  $SU(3)$  which is given by  $T_a = \frac{\lambda_a}{2}$  where  $\lambda_a$  are the 8 Gell-Mann matrices.

To illustrate the features of an non-abelian gauge symmetry we will construct a simple  $SU(2)$  invariant Lagrangian consisting of the a gauge field and a single  $SU(2)$  left handed doublet. We consider an  $SU(2)$  gauge field given by  $W^\mu = \frac{1}{2}W^{i\mu}\sigma^i$ . This gauge field belongs to the adjoint representation of the theory and transforms which gives the following transformation rule:

$$\begin{aligned} W_\mu(x) \rightarrow W'(x) &= UW_\mu(x)U^\dagger - \frac{i}{g}(\partial_\mu U)U^\dagger \\ &= W_\mu + ig_2[W_\mu, \theta(x)] - \partial_\mu\theta(x), \end{aligned} \quad (2.11)$$



SM Gauge Group	Gauge Field	Field Strength Tensor
$U(1)_Y$	$B_\mu$	$B_{\mu\nu} = \partial_\mu B_\nu - \partial_\nu B_\mu$
SU(2)	$W_\mu = \frac{1}{2}W_\mu^i \sigma^i$	$W_{\mu\nu}^i = \partial_\mu W_\nu^i - \partial_\nu W_\mu^i + g\epsilon^{ijk}W_\mu^j W_\nu^k$
SU(3)	$G_\mu = \frac{1}{2}G_\mu^a T^a$	$G_{\mu\nu}^a = \partial_\mu G_\nu^a - \partial_\nu G_\mu^a + gf^{abc}G_\mu^b G_\nu^c$

Table 2.1.: SM gauge symmetries and their corresponding gauge fields.

which implies the components of  $W_\mu$  must transform as

$$W_\mu^i(x) \rightarrow W^{i\mu} - [\delta^{ac}\partial_\mu - ig_2 W_\mu^b (J_A^b)^{ac}] w(x)^c. \quad (2.12)$$

Next we consider the an SU(2) left handed doublet that will be introduce into our Lagrangian:

$$\Psi = \begin{pmatrix} \psi_{1L} \\ \psi_{2L} \end{pmatrix} \quad (2.13)$$

which must have the following transformation law

$$\Psi(x) \rightarrow \Psi' = e^{-ig_2 J^i w^i(x)} \Psi(x) \quad (2.14)$$

where again  $i$  is summed from 1 to three. As before, in order to create a  $SU(2)$  invariant Lagrangian, we need define a gauge invariant derivative called the covariant derivative:

$$D_\mu = \partial_\mu - ig_2 W^\mu = \partial_\mu - ig_2 W^{i\mu} J^i. \quad (2.15)$$

Using these transformation laws an SU(2) invariant Lagrangian can be written as

$$\mathcal{L} = -\frac{1}{4}W_{\mu\nu}^i W^{i\mu\nu} + i\bar{\Psi}\gamma_\mu D^\mu \Psi \quad (2.16)$$

where  $W_{\mu\nu}^a$  is the field strength tensor and is given by

$$W_{\mu\nu}^i = \partial_\mu W_\nu^i - \partial_\nu W_\mu^i + g\epsilon^{ijk}W_\mu^j W_\nu^k. \quad (2.17)$$

The last term in the field strength tensor occurs due to the symmetry being non-abelian. A summary of the SM gauge groups and their gauge fields can be found in table 2.1.

## 2.2 Particle Content of the Standard Model

There are two main types of particles within the SM leptons and quarks. Leptons are spin  $\frac{1}{2}$  particles which are  $SU(3)$  (color) singlets. Leptons only interact under electroweak force and not the strong force. Quarks are  $\frac{1}{2}$  part  $SU(3)$  color triplets which interact with electroweak force and the strong force. In the SM both quarks and leptons have three generations (three copies of the representation). Similar to gauge bosons quark and leptons can not have mass terms. This is due to the fact that we can not write any gauge group singlet in any of the products. The generation of the particle will be represented in this thesis by a subscript  $i$  running from 1 to 3. The particles with their  $SU(3) \times SU(2) \times U(1)$  charges are listed in table 2.2.

Multiplets	$SU(3)_c \otimes SU(2)_L \otimes U(1)_Y$	Particle
Quarks	$(\mathbf{3}, \mathbf{2}, \frac{1}{6})$	$q_{iL} = \begin{pmatrix} u_{iL} \\ d_{iL} \end{pmatrix}$
	$(\mathbf{3}, \mathbf{1}, \frac{2}{3})$	$u_{iR}$
	$(\mathbf{3}, \mathbf{1}, -\frac{1}{3})$	$d_{iR}$
Leptons	$(\mathbf{1}, \mathbf{2}, -\frac{1}{2})$	$l_{iL} = \begin{pmatrix} \nu_{iL} \\ e_{iL} \end{pmatrix}$
	$(\mathbf{1}, \mathbf{1}, -1)$	$e_{iR}$

Table 2.2.: Particle content of the standard model

## 2.3 Electroweak Symmetry Breaking

As mentioned in the introduction of this chapter the  $SU(2) \times U(1)_Y$  symmetry of the standard model is spontaneously broken and a residual  $U(1)_Q$  symmetry associated with electromagnetism remains. This occurs due to the presence of a scalar field,  $\Phi$ , in the  $(2, -\frac{1}{2})$  representation of  $SU(2) \times U(1)$ , where the first number represents its  $SU(2)$  representation and the last number represents its  $U(1)$  charge. It is assumed that this scalar field will acquire a vacuum expectation value (VEV) that will induce masses to some of the gauge bosons and therefore break the  $SU(2) \times U(1)$  symmetry. This scalar particle and its VEV will be responsible for the fermion masses as well.

The complex scalar field  $\phi$  can be written as

$$\Phi = \begin{pmatrix} \phi^+ \\ \phi^0 \end{pmatrix} \quad (2.18)$$

A covariant derivative for this field is given by

$$(D_\mu \Phi)_i = \partial_\mu \Phi_i - i [g_2 W_\mu^a J^a + g_1 B_\mu y]_i^j \Phi_j \quad (2.19)$$

where  $J^a = \frac{1}{2} \sigma^a$  ( $\sigma^a$  being the Pauli matrices) and  $Y$  is the hypercharge of the Higgs which is equal to  $\frac{1}{2}$ . It will be useful to expand the gauge portion  $g_2 W_\mu^a J^a + g_1 B_\mu y$  into matrix form:

$$g_2 W_\mu^a J^a + g_1 B_\mu y = \frac{1}{2} \begin{pmatrix} g_2 W_\mu^3 - g_1 B_\mu & g_2 (W_\mu^1 - iW_\mu^2) \\ g_2 (W_\mu^1 + iW_\mu^2) & -g_2 W_\mu^3 - g_1 B_\mu \end{pmatrix} \quad (2.20)$$

The Lagrangian for these gauge fields and their interaction with the Higgs field can be written as

$$\mathcal{L} = -\frac{1}{4} W_{\mu\nu}^i W^{i\mu\nu} - \frac{1}{4} B^{\mu\nu} B_{\mu\nu} + (D_\mu \Phi)^\dagger (D^\mu \Phi) - V(\Phi^\dagger \Phi) \quad (2.21)$$

where  $V(\Phi^\dagger \Phi)$  can be viewed as a potential for the Higgs boson of this Lagrangian.  $V(\Phi^\dagger \Phi)$  is defined as

$$V(\Phi^\dagger \Phi) = \frac{1}{4} \lambda \left( \Phi^\dagger \Phi - \frac{1}{2} v^2 \right)^2 \quad (2.22)$$

with this potential the complex scalar doublet  $\Phi$  gets a VEV defined by

$$\langle 0 | \Phi | 0 \rangle = \frac{1}{\sqrt{2}} \begin{pmatrix} 0 \\ v \end{pmatrix} \quad (2.23)$$

In all reality this is only a classical approximation for the VEV. To get a better approximation we need to include quantum loop corrections and higher order diagrams, the potential that includes these effects is called the effective potential. It is these quantum corrections that will cause trouble when one calculates the Higgs mass and lead to the gauge hierarchy problem.

A scalar field in the representation  $(2, -\frac{1}{2})$  should have four degrees of freedom. However,

in order to simplify this we work in the unitary gauge in which three of the degrees of freedom are gauged away. In other gauges these extra degrees of freedom are eaten by the gauge bosons which give them the extra degree of freedom needed in order to be massive. In this gauge we define the Higgs vacuum solution the Higgs doublet as

$$\Phi = \frac{1}{\sqrt{2}} \begin{pmatrix} 0 \\ v + h(x) \end{pmatrix} \quad (2.24)$$

where  $v$  is the VEV of the doublet and  $h(x)$  is the expansion around the vacuum corresponding to a physical particle known as the Higgs boson. Now we will focus on the kinetic term for the complex scalar field which will lead to the gauge bosons masses. If we input the VEV we end up with the following term in the Lagrangian:

$$\mathcal{L}_{mass} = -1/8v^2 \begin{pmatrix} 0 & v \end{pmatrix} \begin{pmatrix} g_2 W_\mu^3 - g_1 B_\mu & g_2 (W_\mu^1 - iW_\mu^2) \\ g_2 (W_\mu^1 + iW_\mu^2) & -g_2 W_\mu^3 - g_1 B_\mu \end{pmatrix} \begin{pmatrix} 0 \\ v \end{pmatrix} \quad (2.25)$$

which results in three massive gauge bosons. Two of these gauge bosons are charged under the electromagnetic residual symmetry. To simplify the mass eigenstates of these gauge bosons we define the Weinberg angle (weak mixing angle) as

$$\theta_w = \tan^{-1} \left( \frac{g_1}{g_2} \right) \quad (2.26)$$

Using the Weinberg angle the massive gauge bosons are defined as

$$W_\mu^\pm = \frac{1}{\sqrt{2}} (W_\mu^1 \mp iW_\mu^2) \quad \text{with mass} \quad M_W = \frac{g_2 v}{2} \quad (2.27)$$

$$Z_\mu = \cos(\theta_W) W_\mu^3 - \sin(\theta_W) B_\mu \quad \text{with mass} \quad M_z = \frac{M_W}{\cos(\theta_W)} \quad (2.28)$$

$$A_\mu = \sin(\theta_W) W_\mu^3 + \cos(\theta_W) B_\mu \quad \text{with mass} \quad M_A = 0. \quad (2.29)$$

The reason  $A_\mu$  remains massless is due to it being the gauge boson that is part of the residual electromagnetic  $U(1)_q$  symmetry.

This electroweak symmetry breaking is also responsible for fermion masses. A gauge

invariant interaction of the first generation of leptons with the Higgs scalar is given by

$$\mathcal{L}_{leptons} = -Y_{iL}\bar{l}_{iL}\Phi e_{iR} \quad (2.30)$$

where  $Y_{iL}$  is the Yukawa couplings to a right handed electron,  $e_R$ . When we input the VEV of the complex scalar doublet we end up with a mass term for the electron proportional to its Yukawa coupling.

In the case of the quarks the most general Yukawa Lagrangian that preserves the gauge symmetry can be written as

$$\mathcal{L}_{quarks} = -Y_{dij}\bar{q}_{iL}\Phi d_{jR} - Y_{uij}\bar{q}_{iL}i\sigma_2\tilde{\Phi}u_{jR}, \quad (2.31)$$

where  $\tilde{\Phi} = i\sigma_2\Phi^*$ , the  $Y_{dij}$  and  $Y_{uij}$  are complex Yukawa matrices that are not in general diagonal in flavor space. To diagonalize these matrices and place the Lagrangian in terms of mass eigenstates we can make the following unitary transformations on the fields:

$$\begin{aligned} d'_{Li} &= D_{Lij}d_{Lj}, & u'_{Li} &= U_{Lij}d_{Lj}, \\ d'_{Ri} &= D_{Rij}d_{Rj} & u'_{Ri} &= U_{Rij}d_{Rj}. \end{aligned} \quad (2.32)$$

After this diagonalization the down type quarks and up type quarks have masses proportional to their Yukawa coupling in the same way the leptons did. This diagonalization of the Yukawas will leave the kinetic terms the same but will cause the charged weak currents to be flavor violating (mixing between generations).

## 2.4 Hierarchy Problem

Combined data from the ATLAS and CMS collaborations found a mass of 125.09 GeV for the Higgs boson [4]. This measured mass of the Higgs boson includes all radiative corrections and therefore is not the bare mass of the particle that appears in the Lagrangian. This is a problem since the Higgs mass is not stable against quantum corrections and by expectation it's mass should be quite large.

Consider the Higgs boson coupling to the top quark which is described by the Lagrangian

$$\mathcal{L} = -\frac{y_t}{\sqrt{2}}H\bar{t}t, \quad (2.33)$$

where  $y_t$  is the corresponding Yukawa coupling of the top quark to the Higgs field,  $H$  is the Higgs field and  $t$  is a top quark field. The Yukawa coupling  $y_t$  for the case above is  $y_t = \frac{\sqrt{2}m_t}{v} = \frac{173\sqrt{2}}{246} \approx 1$ . This leads to a one loop correction to the Higgs Mass as seen in Fig.(2.1).

The correction to the Higgs mass by the top quark radiative correction can be calculated by using the Feynman rules on the above diagram Fig.(2.1) and integrating over all internal momenta. The resulting correction is given by

$$\begin{aligned} \delta m_H^2 &= -\frac{y_t^2}{2}Tr \int d^4l \frac{i(\not{l} + m_t)}{\not{l}^2 - m_t^2 + i\epsilon} \frac{i(\not{l} + m_t)}{\not{l}^2 - m_t^2 + i\epsilon} \\ &= -\frac{y_t^2}{8\pi^2} \int_{m_t^2}^{\Lambda_{new}^2 + m_t^2} dq \left( 1 - \frac{3m_t^2}{q} + \frac{2m_t^4}{q^2} \right) \\ &\approx -\Lambda_{new}^2 + 3m_t^2 \ln \left( \frac{\Lambda_{new}^2}{m_t^2} \right) \end{aligned} \quad (2.34)$$

where  $\Lambda_{new}$  is a cutoff scale in which the new physics appears. Since the standard model does not include gravity then new physics must appear at higher energies.

One possible scale is the scale at which gravitational interactions become strong which is often referred to as the Planck scale,  $\Lambda_{new} = M_p = 1.2 \times 10^{19}$  GeV. If we assume the cutoff is indeed the Planck mass then in order to achieve a measured Higgs mass of a 125 GeV there would have to be a cancellation on the order of  $10^{38}$  decimal places between the tree level Higgs mass and the quantum corrections. This high level accuracy is very unusual and is often referred to as the ‘gauge hierarchy problem’. Another way to state this problem is the question on why gravity is so weak compared to the other forces.

Instead of the cutoff method used above we can use dimensional regularization in which no quadratic divergence is present. This is due to the fact that dimensional regularization treats all divergences the same. However, we still are going to have an issue with the Higgs mass in both cases since it will still quadratically sensitive to the existence of the mass of

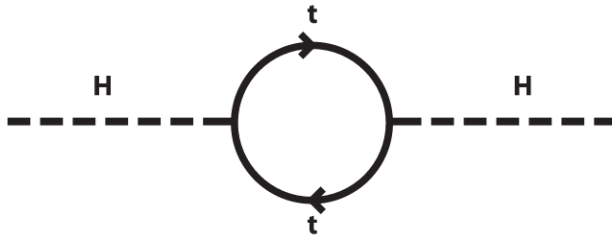


Fig. 2.1.: Feynman diagram of top loop correction to Higgs boson propagator

new heavy particle.

For example consider a new heavy complex scalar particle (N) whose interaction Lagrangian with the Higgs can be written as

$$\mathcal{L} = \lambda_N |H|^2 |N|^2. \quad (2.35)$$

If we renormalize this using dimensional regularization, we obtain only the logarithmic divergence as

$$\delta m_H^2 = \frac{\lambda_N}{16\pi^2} \left( -2m_N^2 \log \left( \frac{\Lambda}{m_N} \right) \right). \quad (2.36)$$

Similar terms occur even in the case that new massive particles don't directly couple with the Higgs boson as long as they and share a gauge interaction with the Higgs boson [15]. Theories that include gravity often include such heavy particles. For example string theory introduce many new heavy particles that would still lead to a hierarchy which would require some degree of fine tuning.

Similar corrections to the heavy gauge boson and fermion propagators don't result in such corrections. The quantum corrections to the SM fermions and massive gauge bosons are proportional to the mass of the particle itself and not to those of new particles. The reason these masses stay small is due to an increased symmetry in the massless limit of both cases. For example if the fermion mass would go to zero we would have an new chiral symmetry of the theory. Similarly in the case of gauge bosons the gauge symmetry is restored in the massless limit.

If one just accepts that the standard model needs this high level of fine tuning between parameters which we still run into an issue when we consider the running of the Higgs

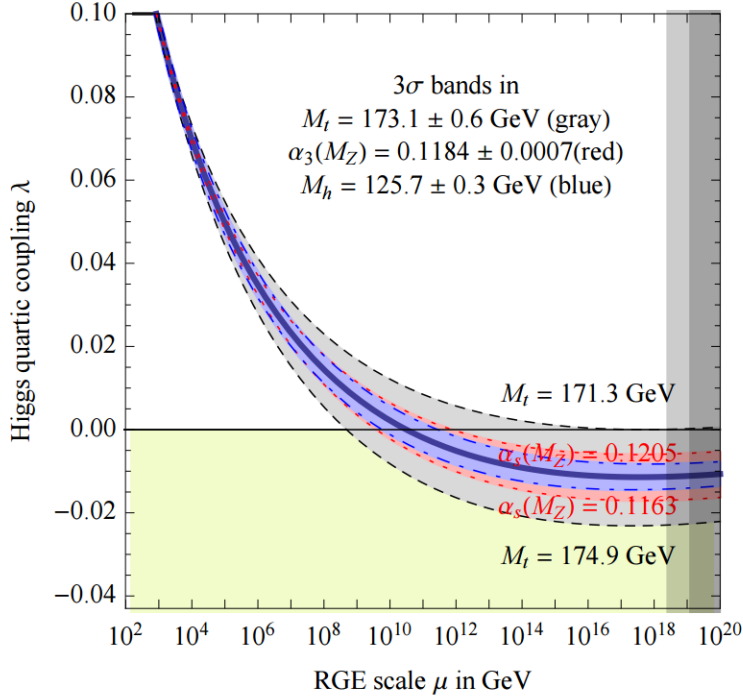


Fig. 2.2.: Higgs Quartic coupling running at next-to-next to leading order propagator. This figure is from Ref. [1].

boson quartic coupling. In [1] the authors have calculated the Higgs boson quartic coupling renormalization group equations at next-to-next-to-leading order. In Fig. 2.2 it can be seen that as the quartic coupling runs towards higher energies it goes negative at about  $10^{10}$  GeV. This presents an issue since it implies that our vacuum isn't the true vacuum [16]. This electroweak vacuum instability may not be a problem, since the lifetime of our vacuum is estimated to be much longer than the age of the universe (meta-stability bound). In order to avoid this issue one would expect new physics before such high energies that would keep the quartic coupling from becoming negative.

The hierarchy problem and electroweak vacuum stability problem can be avoided by introducing some new physics at energy scales below the Planck mass. One such solution is supersymmetry in which for each fermion or boson there are bosonic or fermionic super partners [17]. These super partners also induce their own quantum corrections which result in the cancellation such that the quadratic sensitivity to new physics scales doesn't occur.



There are several solutions that involving using extra dimensions. One idea is the use of large extra dimensions. For example in the ADD model or large extra dimensions the Planck scale is actually much lower and only appears large due to the fact that gravity is propagating in this extra dimension [18]. Another example is the Randall Sundrum model [19]. In this model a 5D space-time is used but the extra dimension is warped. This warping explains the hierarchy between the electroweak and Planck scales .

Another way to avoid the hierarchy problem is by having the Higgs being protected by a higher dimensional gauge symmetry. One such model is gauge Higgs unification (GHU) where the Higgs boson is embedded into a higher dimensional gauge field. The higher dimensional gauge symmetry of the model protects the Higgs mass at high energies [20]. The 4D point of view is that many KK modes will be introduced which will keep the Higgs mass stable against quantum corrections. This is the method that we will be concerned with in this dissertation

### 3 SU(3) × U(1)' GHU MODEL

In this chapter we begin by investigating the effects of compactifying an extra dimension on the physics of the fields within it. Then we introduce a toy model of gauge Higgs unification in 5D using the  $SU(3)$  gauge group [21]. In the final sections we discuss ways to make this model realistic.

#### 3.1 Kaluza Klein Compactification

To compactify an extra dimension means to imagine that the extra dimension takes some finite shape, such that traveling along the extra dimension will quickly return one to the origin. For an example consider an  $M_4 \times S_1$  topology, where  $M_4$  is the usual 4D Minkowski space and  $S_1$  (the extra dimension) is compactified on a circle of radius  $R$ . Let  $x^u$  represent the coordinates of  $M_4$  and  $y$  represent the coordinate of  $S_1$ . The way to think about this topology is that at every point in 4D space-time there exists a circle of radius  $R$  orthogonal to it. This compactification imposes a periodic boundary condition on the extra dimensional coordinate  $y$  such that it is invariant under the transformation  $y \rightarrow y + 2\pi R$ . Now assume for simplicity that a scalar field  $\Phi(x^u, y)$  exists in this space-time topology. The invariance of  $y$  under the transformation  $y \rightarrow y + 2\pi R$  from the  $S_1$  compactification imposes a periodic boundary condition on the scalar field such that  $\Phi(x^u, y) = \Phi(x^u, y + 2\pi R)$ . This boundary condition implies that 5D scalar field can be decomposed into orthogonal states using the following mode expansion (Fourier decomposition along the extra dimension  $y$ ):

$$\Phi(x^u, y) = \frac{1}{\sqrt{2\pi R}} \sum_{n=-\infty}^{\infty} \Phi_n(x^u) e^{iny/R}. \quad (3.1)$$

A 5D free scalar which is a solution to the 5D Klein-Gordon equation has the following action

$$S_5 = \frac{1}{\sqrt{2\pi R}} \int d^4x \int_0^{2\pi R} dy \left[ \frac{1}{2} (\partial_M \Phi)^* (\partial_M \Phi) - \frac{1}{2} m^2 \Phi^* \Phi \right], \quad (3.2)$$

where  $m$  is the mass of the 5D scalar field  $\Phi$  and  $M$  is the five dimensional space-time index.  $M = 0, 1, 2, 3$  correspond to the ordinary Minkowski space-time coordinates  $x^u$  and  $M = 5$  corresponds to the coordinate  $y$  of the compactified dimension. The mode expansion from equation 3.1 is inserted into equation 3.2 and results in the action:

$$\begin{aligned}
S_5 = & \frac{1}{\sqrt{2\pi R}} \int d^4x \int_0^{2\pi R} dy \frac{1}{2} \sum_{mn} \partial_u \Phi_M^* \partial^u \Phi_N e^{\frac{i(n-m)y}{R}} \\
& - \frac{1}{2} \sum_{mn} \left( \frac{-im}{R} \right) \left( \frac{in}{R} \right) \Phi_m^* \Phi_n e^{\frac{i(n-m)y}{R}} \\
& - \frac{1}{2} m_0^2 \sum_{mn} \Phi_m^* \Phi_n e^{\frac{i(n-m)y}{R}}.
\end{aligned} \tag{3.3}$$

This can be simplified since that the modes of the expansion are orthogonal, which is displayed by the equation below

$$\int_0^{2\pi R} e^{\frac{i(n-m)y}{R}} = 2\pi R \delta_{mn}. \tag{3.4}$$

The integration can now be performed easily over the compactified extra dimension giving the action

$$S_4 = \int d^4x \frac{1}{2} \sum_n \partial_u \Phi_n^* \partial^u \Phi_n - \frac{1}{2} \sum_n \left( m^2 + \frac{n^2}{R^2} \right) \Phi_n^* \Phi_n. \tag{3.5}$$

The above equation is just the action of an infinite tower of 4-Dimensional Klein-Gordon fields with masses given by

$$m_n^2 = m^2 + \frac{n^2}{R^2} \tag{3.6}$$

where  $n$  corresponds to the quantum number of the quantized five dimensional momentum,  $p_5 = n/R$ . So any particle which is allowed to propagate through these higher compactified extra dimensions will obtain a KK mass spectrum. This is the case for any compactification.

### 3.2 SU(3) Toy Model

The smallest gauge group in which we can embedded both the  $U(1)$  and  $SU(2)$  gauge fields of the standard model is  $SU(3)$ . In this section we will consider a toy model based on a 5D GHU model in which the fifth dimension is compactified on an  $S^1/Z^2$  orbifold shown

in figure 3.1. This compactification creates two fixed points at  $y = 0$  and  $y = \pi R$  where  $R$  can be considered the radius of the extra dimension. The value  $\frac{1}{R}$  is often referred to as the compactification (KK) scale, often denoted  $m_{KK}$ . The 5D components of the  $SU(3)$  gauge field will appear as just normal scalars in four dimensions and therefore is where we will embed the Higgs doublet and its hermitian conjugate. The basics of such a model are discussed in [21].

The  $SU(3)$  symmetry is broken to  $SU(2) \times U(1)$  by  $S^1/Z^2$  orbifold compactification by assigning non-trivial parities to the fermion and gauge fields. In 5D fermions are vector-like meaning they can't be broken into left and right handed chiral fields. This is an issue since the SM is a chiral theory. One way to get around this is by assigning non-trivial parities to the left and right components which removes some of the zero modes of these components.

At tree level one is forbidden to write a Higgs mass term due to the  $SU(3)$  gauge symmetry. However, since the  $SU(3)$  symmetry will be broken into  $SU(2) \times U(1)$  by choosing non-trivial parities then they will obtain a vacuum expectation value through radiative corrections at low energies. The remaining  $SU(2) \times U(1)$  symmetry is broken into the electromagnetic symmetry  $U(1)_Q$  by the vacuum expectation value of the Higgs doublet embedded into this  $SU(3)$  gauge field.

The 5D  $SU(3)$  Lagrangian with a  $SU(3)$  triplet fermion  $\Psi$  is given by

$$\mathcal{L} = -\frac{1}{2}Tr(F^{MN}F_{MN}) + i\bar{\Psi}\not{D}\Psi \quad (3.7)$$

where  $M, N = 0, 1, 2, 3, 5$  and

$$\not{D} = \Gamma^M (\partial_M - ig_5 A_M) \quad \Gamma^M = (\gamma^\mu, i\gamma^5), \quad (3.8)$$

$$A_M = A_M^a \frac{\lambda^a}{2} (\lambda^a : \text{Gell-Mann Matrices}), \quad (3.9)$$

$$F_{MN} = \partial_M A_N - \partial_N A^M - ig_5 [A_M, A_N] \quad (3.10)$$

$$\psi = \begin{pmatrix} \psi_1 \\ \psi_2 \\ \psi_3 \end{pmatrix}. \quad (3.11)$$

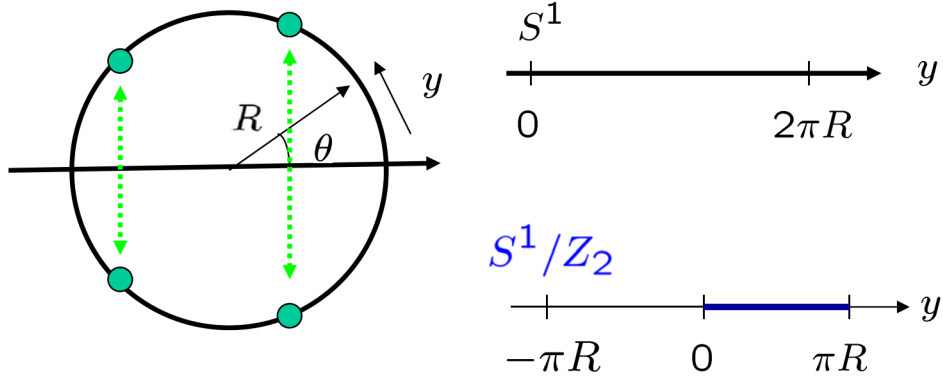


Fig. 3.1.: An illustration of an  $S^1/Z_2$  orbifold.

For this toy model we consider periodic gauge fields which imply that at each fixed point of the 5th dimension ( $y = 0, y = \pi R$ ) these gauge fields must have the same parity at the two fixed points. The two options of the parity for these gauge files are  $(+, +)$  and  $(-, -)$ . Gauge fields with the  $(+, +)$  parity assignment have even parities at both fixed points  $y = 0$  and  $y = \pi R$ . Similarly gauge fields with the  $(-, -)$  parity assignment have odd parity at both fixed points. Only fields with  $(+, +)$  parity have zero modes. This is also true for periodic fermions which will be discussed later.

So in order to get the standard model at the zero mode level we consider the following parity assignments for the gauge fields,

$$A_\mu = \begin{pmatrix} (+, +) & (+, +) & (-, -) \\ (+, +) & (+, +) & (-, -) \\ (-, -) & (-, -) & (+, +) \end{pmatrix}, \quad A_5 = \begin{pmatrix} (-, -) & (-, -) & (+, +) \\ (-, -) & (-, -) & (+, +) \\ (+, +) & (+, +) & (-, -) \end{pmatrix}. \quad (3.12)$$

Under the given boundary conditions and symmetries of the  $S^1/Z^2$  compactification we get the following KK mode expansions for the gauge fields of  $(+, +)$  or  $(-, -)$  parity:

$$A_{\mu,5}^{(+,+)}(x, y) = \frac{1}{\sqrt{2\pi R}} \left[ A_{\mu,5}^{(0)}(x) + \sqrt{2} \sum_{n=1}^{\infty} A_{\mu,5}^{(n)}(x) \cos(ny/R) \right], \quad (3.13)$$

$$A_{\mu,5}^{(-,-)}(x, y) = \frac{1}{\sqrt{\pi R}} \sum_{n=1}^{\infty} A_{\mu,5}^{(n)}(x) \sin(ny/R). \quad (3.14)$$

This allows us to embed the SM gauge bosons into the zero modes of the  $SU(3)$  Gauge field as follows

$$A_\mu^{(0)} = \frac{1}{2} \begin{pmatrix} W_\mu^3 + \frac{B_\mu}{\sqrt{3}} & \sqrt{2}W_\mu^+ & 0 \\ \sqrt{2}W_\mu^- & -W_\mu^3 + \frac{B_\mu}{\sqrt{3}} & 0 \\ 0 & 0 & -\frac{2}{\sqrt{3}}B_\mu \end{pmatrix}, \quad A_5^{(0)} = \frac{1}{\sqrt{2}} \begin{pmatrix} 0 & 0 & h^+ \\ 0 & 0 & h^0 \\ h^- & h^{0*} & 0 \end{pmatrix}. \quad (3.15)$$

Now we can write an  $SU(3)$  triplet fermion in 4D as follows.

$$\psi = \begin{pmatrix} \psi_{1L} + \psi_{1R} \\ \psi_{2L} + \psi_{2R} \\ \psi_{3L} + \psi_{3R} \end{pmatrix} \quad (3.16)$$

Before we assign parities to these particles there is one little caveat. In order to get a solution to the 5D Dirac equation the left and right components of each vector-like fermion must have opposite parities. Using this knowledge we choose the parity assignments as followed

$$\psi = \begin{pmatrix} \psi_{1L}(+,+) + \psi_{1R}(-,-) \\ \psi_{2L}(+,+) + \psi_{2R}(-,-) \\ \psi_{3L}(-,-) + \psi_{3R}(+,+) \end{pmatrix} \quad (3.17)$$

Under the given boundary conditions and symmetries of the  $S^1/Z^2$  compactification we get the following KK expansions for the periodic fermions fields of  $(+,+)$  or  $(-,-)$  parity:

$$\begin{aligned} \psi_{1L,2L,3R}^{(+,+)}(x,y) &= \frac{1}{\sqrt{2\pi R}} \left[ \psi_{1L,2L,3R}^{(0)}(x) + \sqrt{2} \sum_{n=1}^{\infty} \psi_{1L,2L,3R}^{(n)}(x) \cos(ny/R) \right], \\ \psi_{3L,1R,2R}^{(-,-)}(x,y) &= \frac{1}{\sqrt{\pi R}} \sum_{n=1}^{\infty} \psi_{3L,1R,2R}^{(n)}(x) \sin(ny/R). \end{aligned} \quad (3.18)$$

This allows the following embedding of the standard model up and down type quarks at zero

mode level as follows

$$\psi = \begin{pmatrix} u_L \\ d_L \\ d_R \end{pmatrix} \quad (3.19)$$

An effective 4D theory can be found by integrating the extra dimensional variable in the 5D theory between  $y = 0$  and  $y = \pi R$ . A chiral rotation has been used to remove the  $i\gamma_5$  before such integration. We define the neutral Higgs component  $h^0$  as  $h^0 = \frac{h+v}{\sqrt{2}}$  where  $v$  is vacuum expectation value of the Higgs field which breaks the  $SU(2) \times U(1)$  symmetry. Under these conditions the 4D effective Lagrangian for fermions and zero mode gauge field interactions is given by

$$\begin{aligned} \mathcal{L}_{4D} = & \sum_{n=1}^{\infty} (\bar{\psi}_1^{(n)}, \bar{\psi}_2^{(n)}, \bar{\psi}_3^{(n)}) i\gamma^\mu \partial_\mu \begin{pmatrix} \psi_1^{(n)} \\ \psi_2^{(n)} \\ \psi_3^{(n)} \end{pmatrix} \\ & + \frac{g_2}{2} (\bar{\psi}_1^{(n)}, \bar{\psi}_2^{(n)}, \bar{\psi}_3^{(n)}) \begin{pmatrix} W_\mu^3 + \frac{B_\mu}{\sqrt{3}} & \sqrt{2}W_\mu^+ & 0 \\ \sqrt{2}W_\mu^- & -W_\mu^3 + \frac{B_\mu}{\sqrt{3}} & 0 \\ 0 & 0 & -\frac{2}{\sqrt{3}}B_\mu \end{pmatrix} i\gamma^\mu \begin{pmatrix} \psi_1^{(n)} \\ \psi_2^{(n)} \\ \psi_3^{(n)} \end{pmatrix} \\ & - (\bar{\psi}_1^{(n)}, \bar{\psi}_2^{(n)}, \bar{\psi}_3^{(n)}) \begin{pmatrix} m_n & 0 & 0 \\ 0 & m_n & -(M_W + gh) \\ 0 & -(M_W + gh) & m_n \end{pmatrix} \begin{pmatrix} \psi_1^{(n)} \\ \psi_2^{(n)} \\ \psi_3^{(n)} \end{pmatrix} \\ & + \bar{d} (i\gamma^\mu - M_w - g_2 h) d + i\bar{u}_L \gamma^\mu u_L \\ & + g_2 (\bar{u}_L \gamma^\mu d_L W_\mu^+ + \bar{d}_L \gamma^\mu d_L W_\mu^-) \\ & + \frac{g_2}{2} (\bar{u}_L \gamma^\mu d_L - \bar{d}_L \gamma^\mu d_L) W_\mu^3 \\ & + \frac{\sqrt{3}g_2}{6} (\bar{u}_L \gamma^\mu u_L + \bar{d}_L \gamma^\mu d_L - 2\bar{d}_R \gamma^\mu d_R) B^\mu, \end{aligned} \quad (3.20)$$

where  $g_2 = \frac{g_5}{\sqrt{2\pi R}}$ ,  $m_n = \frac{n}{R}$ , and  $M_w = \frac{g_2 v}{2}$  is the mass of the W boson. In the above it is observed that the up type quark is massless while the bottom type quarks both end up with a mass equal to that of the W boson. This is common in GHU models since the Yukawa couplings are unified with the gauge coupling  $g_2$ . There are methods to allow us to correct

the masses of these particles which will be discussed in future sections.

Another important observation is that the mass matrix for the KK modes have off diagonal entries which means the mass matrix requires diagonalization. We can diagonalize the Lagrangian into the mass eigenstates  $\tilde{\psi}_2^{(n)}, \tilde{\psi}_3^{(n)}$

$$\begin{pmatrix} \psi_1^{(n)} \\ \tilde{\psi}_2^{(n)} \\ \tilde{\psi}_3^{(n)} \end{pmatrix} = U \begin{pmatrix} \psi_1^{(n)} \\ \psi_2^{(n)} \\ \psi_3^{(n)} \end{pmatrix}, \quad U = \frac{1}{\sqrt{2}} \begin{pmatrix} \sqrt{2} & 0 & 0 \\ 0 & 1 & -1 \\ 0 & 1 & 1 \end{pmatrix}, \quad (3.21)$$

which results in the following mass matrix

$$U \begin{pmatrix} m_n & 0 & 0 \\ 0 & m_n & -M_W \\ 0 & -M_W & m_n \end{pmatrix} U^\dagger = \begin{pmatrix} m_n & 0 & 0 \\ 0 & m_n + M_W & 0 \\ 0 & 0 & m_n - M_W \end{pmatrix}. \quad (3.22)$$

The mass splitting that occurs is a property of the GHU scenario which is not present in models with large extra dimensions. For the KK modes ( $n \geq 1$ ) the Lagrangian in terms of the mass eigenstates is given by

$$\begin{aligned} \mathcal{L}_{\text{fermion}}^{(4D)} &= \sum_{n=1}^{\infty} \left\{ (\bar{\psi}_1^{(n)}, \bar{\psi}_2^{(n)}, \bar{\psi}_3^{(n)}) \right. \\ &\times \begin{pmatrix} i\gamma^\mu \partial_\mu - m_n & 0 & 0 \\ 0 & i\gamma^\mu \partial_\mu - (m_n^+ + \frac{M_W}{v} h) & 0 \\ 0 & 0 & i\gamma^\mu \partial_\mu - (m_n^- - \frac{M_W}{v} h) \end{pmatrix} \begin{pmatrix} \psi_1^{(n)} \\ \tilde{\psi}_2^{(n)} \\ \tilde{\psi}_3^{(n)} \end{pmatrix} \\ &+ \frac{g}{2} (\bar{\psi}_1^{(n)}, \bar{\psi}_2^{(n)}, \bar{\psi}_3^{(n)}) \begin{pmatrix} W_\mu^3 + \frac{\sqrt{3}B_\mu}{3} & W_\mu^+ & W_\mu^+ \\ W_\mu^- & -\frac{W_\mu^3}{2} - \frac{\sqrt{3}B_\mu}{6} & -\frac{W_\mu^3}{2} + \frac{\sqrt{3}B_\mu}{2} \\ W_\mu^- & -\frac{W_\mu^3}{2} + \frac{\sqrt{3}B_\mu}{2} & -\frac{W_\mu^3}{2} - \frac{\sqrt{3}B_\mu}{6} \end{pmatrix} \gamma^\mu \begin{pmatrix} \psi_1^{(n)} \\ \tilde{\psi}_2^{(n)} \\ \tilde{\psi}_3^{(n)} \end{pmatrix} \left. \right\} \end{aligned} \quad (3.23)$$

where  $m_n^+ = m_n + M_W$  and  $m_n^- = m_n - M_W$ .

Another interesting fact about this model is that the SU(3) bulk symmetry does not



forbid us from writing a bulk mass term. So in order to create a mass term it will require us to introduce a pair of SU(3) triplet fields such that the left and right handed components have opposite parity. For example consider an SU(3) triplet,  $\psi_a$  in which the parities have been assigned as follows

$$\psi_a = \begin{pmatrix} \psi_{1L}(+,+) + \psi_{1R}(-,-) \\ \psi_{2L}(+,+) + \psi_{2R}(-,-) \\ \psi_{3L}(-,-) + \psi_{3R}(+,+) \end{pmatrix} \quad (3.24)$$

Then we can introduce another SU(3) triplet,  $\tilde{\psi}_a$  with the following parity assignments

$$\tilde{\psi}_a = \begin{pmatrix} \psi_{1L}(-,-) + \psi_{1R}(+,+) \\ \psi_{2L}(-,-) + \psi_{2R}(+,+) \\ \psi_{3L}(+,+) + \psi_{3R}(-,-) \end{pmatrix} \quad (3.25)$$

This allows the creation of a bulk mass term given by

$$M \left( \tilde{\psi}_a \psi_a + \bar{\psi}_a \tilde{\psi}_a \right). \quad (3.26)$$

There is another way which allows an parity even bulk mass term in which we do not have to introduce another 5D bulk fermion with opposite parity but still conserve  $Z_2$  parity at the brane. This method involves introducing a bulk kink mass. The only issue is that this method changes the wave function for the zero mode and higher KK modes. For an  $SU(3)$  triplet  $\Psi_a$ , one can define a kink mass term as

$$\epsilon(y) M \bar{\Psi}_a \Psi_a, \quad \epsilon(y) = \begin{cases} 1, & \text{if } y > 0. \\ -1, & \text{if } y < 0. \end{cases} \quad (3.27)$$

This introduction of the kink bulk mass will be used later on to help get the correct SM fermion masses.

Another issue with this toy model involves the Weinberg angle. The Weinberg angle at tree level is predicted to be too large by this model [22]. To calculate the Weinberg angle we

need to first find the hypercharge of the Higgs doublet. In this  $SU(3)$  model the hypercharge gauge boson is embedded into  $T^8$ . So we can calculate the hypercharge of the Higgs boson as follows

$$\delta_{U(1)} A_5^0 = g_2 [T^8, A_5^0] = \frac{\sqrt{3}g_2}{2} \begin{pmatrix} 0 & 0 & h^+ \\ 0 & 0 & h^0 \\ -h^- & -h^{0*} & 0 \end{pmatrix}. \quad (3.28)$$

So the hypercharge  $g_y$  of the Higgs boson in this case is  $\sqrt{3}$ . Now putting this in for the formula of the Weinberg angle gives the following

$$\sin^2(\theta_w) = \frac{g_y^2}{g_2^2 + g_y^2} = 3/4. \quad (3.29)$$

The correct value for the Weinberg angle is 0.23 so the Weinberg angle in this theory is too large. In the following sections we discuss ways to create a realistic GHU scenario in 5D by introducing methods that lower the masses of the fermions and introduce a method which allows for the correct Weinberg angle.

### 3.3 Correct Weinberg Angle at Tree Level

As mentioned in the previous section the Weinberg angle in the  $SU(3)$  model is incorrect. A way to achieve the correct Weinberg angle is to add an extra  $U(1)'$  symmetry in the bulk with coupling  $Xg'$ , where  $X$  is the charge of the particles under this new symmetry [22]. The  $U(1)'$  symmetry will not be affected by the orbifold projections. So, the  $SU(3) \times U(1)'$  symmetry is broken by the orbifolding at the zero mode level to  $SU(2) \times U(1)_8 \times U(1)'$ . Now we associate  $U(1)_Y$  as the sum of  $U(1)_8$  and  $U(1)'$ . In the case of charged bulk fermions only the sum of  $U(1)'$  and  $U(1)_8$  gauge bosons is anomaly free and thus is associated with the hypercharge. In this model the electric charge operator is now given by

$$Q = T_3 + \frac{1}{\sqrt{3}}T_8 + X \quad (3.30)$$

where  $T_3$  and  $T_8$  are the associated Gell-Mann matrices and  $X$  is the charge of the particle under this new  $U(1)'$  symmetry.

After the breaking of the  $SU(3)$  symmetry through orbifold compactification and the assignment of non-trivial parities we end up with a gauge field  $B_\mu$  associated with the hypercharge and its orthonormal combination  $A_x$ . These gauge fields are given by

$$B_\mu = \frac{g' A_8 + \sqrt{3} g_2 A'}{\sqrt{3g_2^2 + g'^2}}, \quad A_x = \frac{\sqrt{3} g_2 A_8 - g' A'}{\sqrt{3g_2^2 + g'^2}}. \quad (3.31)$$

Thus the hypercharge coupling is

$$g_Y = \frac{\sqrt{3} g_2 g'}{\sqrt{3g_2^2 + g'^2}}. \quad (3.32)$$

This gives the following result for the Weinberg angle

$$\sin^2(\theta_w) = \frac{g_y^2}{g_2^2 + g_y^2} = \frac{3}{3 + 4 \frac{g_2^2}{g'^2}}. \quad (3.33)$$

In order to get the correct Weinberg angle the coupling  $g'$  must be adjusted such that  $\frac{g_2^2}{g'^2} = 3.014$ .

As mentioned above the  $U(1)_x$  symmetry is anomalous and therefore its mass should be proportional to the cutoff of the theory,  $M_x \propto \Lambda$ . After electroweak symmetry breaking we get a mass mixing between the  $Z$  boson and this new massive gauge boson. However, the large mass of this new gauge boson helps make this effect negligible. In order to achieve a low energy theory we integrate out this heavy gauge boson which will lead to a correction to the electroweak  $\rho$  parameter proportional to  $(\frac{M_z}{\Lambda})^2$ . Current experimental observations place lower bounds on  $\Lambda$  on the order of a couple TeV.

### 3.4 Correct Fermion Mass Spectrum

In the previous section it was observed that the zero mode fermion masses were to large and proportional to the  $W$  boson mass. There are two methods that allow us lower the zero mode fermion masses of the  $SU(3)$  GHU to values which are consistent with the SM. The first method involves giving the 5D fermions a kink bulk mass which localizes the left

and right hand components at different locations along the 5th dimension [23]. The other method involves introducing SM fermions on the brane at one of the fixed points and allowing for mixing with massive bulk fields which share the same quantum numbers [20]. In this dissertation we will only present the first scenario.

As an example consider an  $SU(3)$  triplet given as in eq. 3.24 with the introduction of a bulk kink mass. In this case the Lagrangian for the particle is given by

$$\mathcal{L} = i\bar{\Psi}\not{D}\Psi - \epsilon(y) M\bar{\Psi}\Psi \quad (3.34)$$

where  $\not{D}$  is defined in eq. 3.8. Using the Dirac equation we can solve for the eigenmodes and get the following

$$\psi = \begin{pmatrix} \psi_{1L}(x) f_L^0(y) + \sum_{n=1}^{\infty} \left( \Psi_{1L}^{(n)}(x) f_L^{(n)}(y) + \Psi_{1R}^{(n)} \frac{1}{\sqrt{\pi R}} \sin(M_n y) \right) \\ \psi_{2L}(x) f_L^0(y) + \sum_{n=1}^{\infty} \left( \Psi_{2L}^{(n)}(x) f_L^{(n)}(y) + \Psi_{2R}^{(n)} \frac{1}{\sqrt{\pi R}} \sin(M_n y) \right) \\ \psi_{3R}(x) f_R^0(y) + \sum_{n=1}^{\infty} \left( \Psi_{3R}^{(n)}(x) f_R^{(n)}(y) + \Psi_{3L}^{(n)} \frac{1}{\sqrt{\pi R}} \sin(M_n y) \right) \end{pmatrix}, \quad (3.35)$$

where  $M_n = \frac{n}{R}$  and

$$f_L^0(y) = \sqrt{\frac{M}{1 - e^{-2\pi MR}}} e^{-M|y|} \quad (3.36)$$

$$f_L^n(y) = \frac{M_n}{\sqrt{\pi R} \sqrt{M^2 + M_n^2}} \left[ \cos(M_n y) - \frac{M}{M_n} \epsilon(y) \sin(M_n y) \right] \quad (3.37)$$

$$f_R^0(y) = \sqrt{\frac{M}{e^{2\pi MR} - 1}} e^{M|y|} \quad (3.38)$$

$$f_R^n(y) = \frac{M_n}{\sqrt{\pi R} \sqrt{M^2 + M_n^2}} \left[ \cos(M_n y) + \frac{M}{M_n} \epsilon(y) \sin(M_n y) \right] \quad (3.39)$$

As one can see from these equations the left handed particle is going to be localized around the  $y = 0$  brane while the right handed zero mode is localized around the  $y = \pi R$  brane. The localization of the left and right handed wavefunctions will cause their overlap to be very small which allows us to achieve a realistic fermion mass. Now if we focus for example

on just the  $\psi_2$  component of the triplet we get a 4D effective Yukawa coupling given by

$$\begin{aligned}
Y_2 &= \int_{-\pi R}^{\pi R} g_2 f_L^0(y) f_R^0(y) dy \\
&= g_2 \int_{-\pi R}^{\pi R} \sqrt{\frac{M^2}{(1 - e^{-2\pi MR})(e^{2\pi MR} - 1)}} dy \\
&\approx 2\pi MR g_2 e^{-\pi MR}
\end{aligned}$$

with  $Y_2 \leq g_2$ . By tuning the bulk mass for a given compactification scale we can achieve  $Y_2 \ll g_2$  which in turn would give us  $m_2 \ll M_W$ . This works well except for the case of the top Quark. In order to get the correct top quark mass we have to introduce a hierarchy between the compactification scale and the bulk mass which will require a large amount of 'fine tuning'.

As we just discussed, fermions in the GHU scenario have a mass originally on the order of the mass of the W boson. An upper limit can be placed on these quarks masses which depends on the representation in which they are embedded in. Thus if we embed the fermions in a representation of rank  $k$ , number of indices the representation has in tensor notation, the upper bound on a mass for fermions in that representation is given by

$$m_f \leq \sqrt{k} M_W \tag{3.40}$$

where  $m_f$  is the fermion mass under consideration and  $M_W$  is the W boson mass [24].

In order to get the correct mass for the top quark we would need a minimum of a factor of 2 out front. The other 10 GeV results from QCD quantum corrections to the top mass [25]. Thus a possible solution is to embed the top quark in a higher representation of  $SU(3)$ . The representation we need to use has to have at least 4 indices ( $k$ ). One such representation is the  $\mathbf{15}^*$ -plet of  $SU(3)$ , where the  $*$  implies the complex conjugate. In order to be able to embed the top quark into the 15-plet, the bulk 15-plet fermion in the 5D Lagrangian must be assigned to a bulk  $U(1)'$  charge of  $-\frac{2}{3}$ . This  $SU(3)$  symmetry will be broken by the boundary conditions.

Thus the  $SU(3)$   $\mathbf{15}^*$ -plet decomposes into its  $SU(2) \times U(1)$  subgroup as follows

$$\mathbf{15}^* = \mathbf{1}_{\frac{2}{3}} \oplus \mathbf{2}_{\frac{1}{6}} \oplus \mathbf{3}_{-\frac{1}{3}} \oplus \mathbf{4}_{-\frac{1}{6}} \oplus \mathbf{5}_{-\frac{2}{3}} \quad (3.41)$$

where the  $*$  means the complex conjugate representations, the bold numbers on right hand side list their  $SU(2)$  identification and the numbers in the subscript are the hypercharge with no addition of  $U(1)'$ . The issue is that the orbifold condition will leave many unwanted zero modes of this  $SU(3)$   $\mathbf{15}$ -plet. Actually this occurs in many models where we try to embed the SM fermions in different plets of  $SU(3)$ . To remove these from the theory one can add a localized brane mass term. This involves introducing a particle with the same quantum numbers but opposite chirality on the brane and then having the two match up and create a mass term. This mass term is a free parameter of the theory.

## 4 GAUGE HIGGS CONDITION

In this chapter we will calculate the effective potential for the model presented in chapter 3. To get the VEV of this model one needs to minimize this potential. Even though the 5D theory is non-renormalizable we will get a finite result for the Higgs mass with no quadratic divergence in the 4D effective theory [26]. In the end it will be observed that the quantum corrections to the Higgs mass are proportional to the compactification scale (KK mass scale). Thus if the compactification scale is of the order of 1 TeV the unnatural amount of fine tuning due to the hierarchy problem vanishes.

In many GHU models calculating and minimizing the effective potential to find the correct electroweak symmetry breaking vacuum is a non-trivial task. Instead a model independent approach is developed by viewing the GHU as the UV completion of the standard model. This gauge-Higgs condition will allow us to use the Standard Model RG equations along with any particles that appear below the compactification scale to get an estimate of the Higgs mass in a model independent way. It will be observed that using this method in order to get the correct Higgs boson mass the KK mass scale (compactification scale) would have to be about  $10^{10}$  GeV [27]. Ways to lower the compactification scale will be discussed.

### 4.1 Effective Potential and Higgs Mass in SU(3) Toy Model

As mentioned in previous chapter in the GHU scenario there can not be a Higgs mass at tree level. Instead the Higgs mass must be induced by radiative corrections at low energy. We consider the toy  $SU(3)$  model in chapter 3. In the toy  $SU(3)$  model a triplet bulk fermion with periodic boundary conditions was introduced.

A method to calculate the effective potential by summing all 1-loop diagrams with an arbitrary number of external lines attached is presented in [28]. A method is proposed in [29], which simplifies the calculation greatly. In this method, we calculate the tadpole diagrams which correspond to the first derivative of the effective potential, and integrate it with respect to the scalar field.

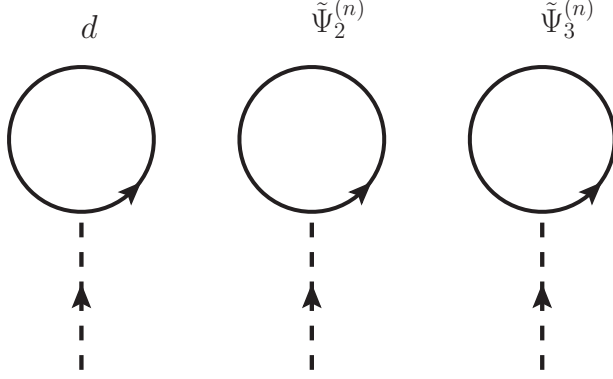


Fig. 4.1.: Tadpoles diagrams contributing to the effective potential

After diagonalization of the SU(3) model in chapter 3, the Lagrangian contained the following terms:

$$\begin{aligned} \mathcal{L} \supset \bar{d} \left( i\gamma^\mu D_\mu - \frac{g_2 h}{2} \right) d + \sum_{n=1}^{\infty} \left[ \overline{\tilde{\Psi}_2^{(n)}} \left( i\gamma^\mu D_\mu - \left( m_n + \frac{g_2 h}{2} \right) \right) \tilde{\Psi}_2^{(n)} \right. \\ \left. + \overline{\tilde{\Psi}_3^{(n)}} \left( i\gamma^\mu D_\mu - \left( m_n - \frac{g_2 h}{2} \right) \right) \tilde{\Psi}_3^{(n)} \right] \end{aligned} \quad (4.1)$$

where  $h$  is the Higgs field. We calculate the tadpole diagrams in Fig. 4.1, which correspond to the first derivative of the effective potential with the substitution of  $h = v$ :

$$\begin{aligned} -i \frac{\partial V_{eff}}{\partial h} \Big|_{h=v} &= \frac{g_2}{2} \text{Tr} \int \frac{d^4 l}{(2\pi)^4} \frac{-\ell + M_W}{\ell^2 + M_W^2} + \sum_{n=1}^{\infty} \text{Tr} \int \frac{d^4 l}{(2\pi)^4} \left[ \frac{-\ell + M_n^+}{\ell^2 + M_n^{+2}} + \frac{-\ell + M_n^-}{\ell^2 + M_n^{-2}} \right] \\ &= 4 \frac{g_2}{2} \int \frac{d^4 l}{(2\pi)^4} \sum_{n=-\infty}^{\infty} \frac{M_n^+}{\ell^2 + M_n^{+2}}, \end{aligned} \quad (4.2)$$

where  $M_n^\pm = (n/R) \pm M_W$ . After performing a Wick rotation, integrating over the solid angle, and making the substitution  $q = \ell^2$  we end up with the following formula,

$$-i \frac{\partial V_{eff}}{\partial h} \Big|_{h=v} = \frac{i}{4\pi^2} \int_0^\infty dq q \sum_{n=-\infty}^{\infty} \frac{M_n^+}{\ell^2 + M_n^{+2}}. \quad (4.3)$$

It is easy to notice that  $\frac{M_n^+}{\ell^2 + M_n^{+2}} = \frac{\partial}{\partial h} \ln(q + M_n^{+2})$ . This now gives the effective potential as



follows:

$$\begin{aligned}
V_{eff}(h) &= -\frac{1}{8\pi^2} \sum_{n=-\infty}^{\infty} \int_0^{\infty} dq q \ln \left( q + \left( \frac{n}{R} + \frac{g_2}{2} h \right)^2 M_n^{+2} \right) \\
&= \frac{3}{16\pi^6 R^4} \sum_{n=1}^{\infty} \frac{\cos(\pi n g R h)}{n^5}.
\end{aligned} \tag{4.4}$$

Note that this potential is finite even though the 5D theory is non-renormalizable. This occurs due to the KK modes that appear in the effective 4D theory. Now we use this effective potential to evaluate the Higgs mass as

$$m_H^2 = \left. \frac{\partial^2 V_{eff}}{\partial h^2} \right|_{h=0} = \frac{3g_2^2}{16\pi^4 R^2} \zeta(3). \tag{4.5}$$

Thus there is no quadratic divergence and the cutoff  $\Lambda$  is now replaced with the compactification scale  $m_{KK} = \frac{1}{R}$ . Thus if the compactification scale is on the order of 1 TeV, then GHU scenario provides a solution to the hierarchy problem.

## 4.2 Deriving the Gauge-Higgs Condition

The actual calculation of the one loop effective potential for the Higgs field is extremely difficult in most cases and at higher loop levels. In a low energy effective theory of this model there will be only down quark chiral modes below the compactification (KK) scale and all heavier particles will be integrated out. Thus we will end up with the Yukawa coupling of the down quark given by

$$\mathcal{L}_Y = -\frac{g_2}{2} h \bar{d} d. \tag{4.6}$$

Now using this Lagrangian we can calculate the contributions to the Higgs potential  $V_{eff}(h)$  due to quantum corrections in this low energy effective theory. These corrections will have UV divergences along with an infrared divergence at  $h = 0$ . Therefore, using the convention adopted in [28] we define the Higgs quartic coupling ( $\lambda(\mu)$ ) at a renormalization scale  $\mu$  as

$$\left. \frac{\partial^4 V_{eff}}{\partial h^4} \right|_{h=\mu} = \lambda(\mu), \tag{4.7}$$

With this definition the Higgs potential in this low energy effective theory can be calculated and is given by

$$V_{eff} = \frac{1}{4!} \left[ \lambda(\mu) - \frac{3}{\pi^2} \frac{g_2^4}{2} \left[ \ln \left( \frac{h^2}{\mu^2} \right) - \frac{25}{6} \right] \right] h^4 \quad (4.8)$$

Now in the previous section we calculated the effective potential from the effective 4D theory. The Higgs VEV is much less than the compactification scale  $m_{KK} = \frac{1}{R}$  which implies that  $\pi g_2 R h \ll 1$ . This will allow us to use the following expansion for the effective potential in the previous section.

$$\sum_{n=1}^{\infty} \frac{1}{n^5} \cos(nx) = \zeta(5) - \frac{1}{2} \zeta(3) x^2 - \frac{1}{48} x^4 \left( \ln(x^2) - \frac{25}{6} \right) + \dots \quad (4.9)$$

After completing the expansion we concentrate on the quartic term which is

$$\begin{aligned} V_{eff}|_{h^4} &= -\frac{3g^4}{768\pi^2} \left( \ln [(\pi g R h)^2] - \frac{25}{6} \right) h^4 \\ &\approx -\frac{g^4}{256\pi^2} \left( \ln \left( \frac{h^2}{m_{KK}^2} \right) - \frac{25}{6} \right) h^4. \end{aligned} \quad (4.10)$$

Now we compare equations 4.8 and 4.10, and find that they are equivalent if we set the renormalization condition as

$$\lambda(m_{KK}) = 0 \quad (4.11)$$

This is the ‘‘gauge-Higgs condition’’ [7]. Thus implies that as we increase to higher energies the 5D gauge symmetry of the model is restored as scales smaller than the volume of the extra dimensions  $2\pi R$ . This will allow us to study the Higgs mass through the RG equations of the Standard Model (plus any exotic particles below the compactification scale) as long as we use the boundary condition that the Higgs quartic coupling must vanish at the compactification scale.

### 4.3 Higgs Mass from the Gauge-Higgs Condition

In our effective theory approach, we can easily evaluate the Higgs boson mass by using the gauge-Higgs condition. We approximated the effective Higgs potential by the quadratic and quartic terms. This means that once the electroweak symmetry breaking is achieved, the physical Higgs boson mass is given by  $m_H = \lambda v^2$ , where  $v = 246$  GeV is the Higgs VEV.

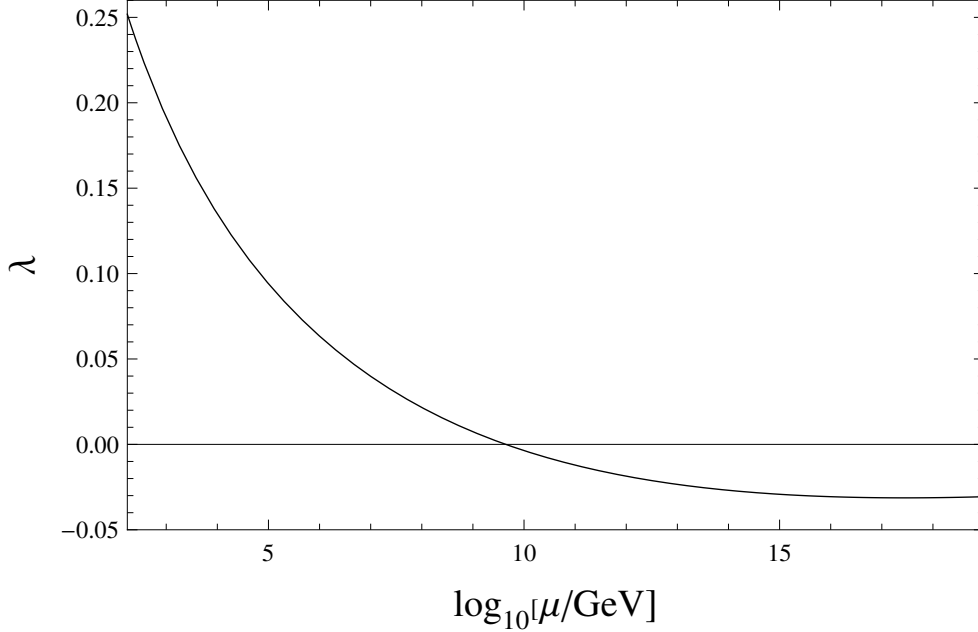


Fig. 4.2.: The RG evolution of the Higgs quartic coupling in the SM for the input of the Higgs boson pole mass  $m_H = 125.09$  GeV.

Therefore, for a fixed compactification scale, we solve RG equation from the compactification scale to the electroweak scale and predict the Higgs boson mass. In the following, we discuss how to reproduce the Higgs boson mass measured at the LHC by unsung the gauge-Higgs condition.

Here, let us assume that only the Standard Model particles appear at energies below the compactification scale. In this case, we evaluate the Higgs boson mass by solving the SM RG equations with the gauge-Higgs condition  $\lambda(m_{KK}) = 0$  at a given compactification scale  $m_{KK}$ . It is easy to reproduce the Higgs boson mass  $m_H = 125.09$  GeV from a combined analysis by the ATLAS and CMS collaborations [4]. Instead of solving the RG equations from high energy to low energy, we extrapolate the Higgs quartic coupling from the electroweak scale to high energies with the input of  $m_h = 125.09$  GeV. As we discussed in chapter 1, RG analysis in the Standard Model shows that the running Higgs quartic coupling becomes negative at the energy around  $10^{10}$  GeV. In our GHU scenario, this energy is interpreted as the compactification scale.

Let us now analyze the RG equations. For the renormalization scale below the compactification scale, all the KK modes are decoupled and we employ the SM RG equations at the

two-loop level [30] For the three SM gauge couplings  $g_i$  ( $i = 1, 2, 3$ ), we have

$$\frac{dg_i}{d \ln \mu} = \frac{b_i}{16\pi^2} g_i^3 + \frac{g_i^3}{(16\pi^2)^2} \left( \sum_{j=1}^3 B_{ij} g_j^2 - C_i y_t^2 \right), \quad (4.12)$$

where the first and second terms in the right hand side are the beta functions at the one-loop and the two-loop levels, respectively, with the coefficients,

$$b_i = \left( \frac{41}{10}, -\frac{19}{6}, -7 \right), \quad B_{ij} = \begin{pmatrix} \frac{199}{50} & \frac{27}{10} & \frac{44}{5} \\ \frac{9}{10} & \frac{35}{6} & 12 \\ \frac{11}{10} & \frac{9}{2} & -26 \end{pmatrix}, \quad C_i = \left( \frac{17}{10}, \frac{3}{2}, 2 \right). \quad (4.13)$$

For contributions from the SM Yukawa coupling to the beta function at the two-loop level, we have considered only the top Yukawa coupling ( $y_t$ ). The RG equation for the top Yukawa coupling is given by

$$\frac{dy_t}{d \ln \mu} = y_t \left( \frac{1}{16\pi^2} \beta_t^{(1)} + \frac{1}{(16\pi^2)^2} \beta_t^{(2)} \right), \quad (4.14)$$

where the one-loop contribution is

$$\beta_t^{(1)} = \frac{9}{2} y_t^2 - \left( \frac{17}{20} g_1^2 + \frac{9}{4} g_2^2 + 8g_3^2 \right), \quad (4.15)$$

while the two-loop contribution is given by

$$\begin{aligned} \beta_t^{(2)} &= -12y_t^4 + \left( \frac{393}{80} g_1^2 + \frac{225}{16} g_2^2 + 36g_3^2 \right) y_t^2 \\ &+ \frac{1187}{600} g_1^4 - \frac{9}{20} g_1^2 g_2^2 + \frac{19}{15} g_1^2 g_3^2 - \frac{23}{4} g_2^4 + 9g_2^2 g_3^2 - 108g_3^4 \\ &+ \frac{3}{2} \lambda^2 - 6\lambda y_t^2. \end{aligned} \quad (4.16)$$

The RG equation for the quartic Higgs coupling is given by

$$\frac{d\lambda}{d \ln \mu} = \frac{1}{16\pi^2} \beta_\lambda^{(1)} + \frac{1}{(16\pi^2)^2} \beta_\lambda^{(2)}, \quad (4.17)$$

with the one-loop beta function,

$$\begin{aligned}\beta_\lambda^{(1)} &= 12\lambda^2 - \left(\frac{9}{5}g_1^2 + 9g_2^2\right)\lambda + \frac{9}{4}\left(\frac{3}{25}g_1^4 + \frac{2}{5}g_1^2g_2^2 + g_2^4\right) \\ &+ 12y_t^2\lambda - 12y_t^4,\end{aligned}\tag{4.18}$$

and the two-loop beta function,

$$\begin{aligned}\beta_\lambda^{(2)} &= -78\lambda^3 + 18\left(\frac{3}{5}g_1^2 + 3g_2^2\right)\lambda^2 - \left(\frac{73}{8}g_2^4 - \frac{117}{20}g_1^2g_2^2 - \frac{1887}{200}g_1^4\right)\lambda - 3\lambda y_t^4 \\ &+ \frac{305}{8}g_2^6 - \frac{289}{40}g_1^2g_2^4 - \frac{1677}{200}g_1^4g_2^2 - \frac{3411}{1000}g_1^6 - 64g_3^2y_t^4 - \frac{16}{5}g_1^2y_t^4 - \frac{9}{2}g_2^4y_t^2 \\ &+ 10\lambda\left(\frac{17}{20}g_1^2 + \frac{9}{4}g_2^2 + 8g_3^2\right)y_t^2 - \frac{3}{5}g_1^2\left(\frac{57}{10}g_1^2 - 21g_2^2\right)y_t^2 \\ &- 72\lambda^2y_t^2 + 60y_t^6.\end{aligned}\tag{4.19}$$

In solving the RG equations, we use the boundary conditions at the top quark pole mass ( $M_t$ ) given in [30]:

$$\begin{aligned}g_1(M_t) &= \sqrt{\frac{5}{3}}\left(0.35761 + 0.00011(M_t - 173.10) - 0.00021\left(\frac{m_W - 80.384}{0.014}\right)\right), \\ g_2(M_t) &= 0.64822 + 0.00004(M_t - 173.10) + 0.00011\left(\frac{m_W - 80.384}{0.014}\right), \\ g_3(M_t) &= 1.1666 + 0.00314\left(\frac{\alpha_s - 0.1184}{0.0007}\right), \\ y_t(M_t) &= 0.93558 + 0.0055(M_t - 173.10) - 0.00042\left(\frac{\alpha_s - 0.1184}{0.0007}\right) \\ &- 0.00042\left(\frac{m_W - 80.384}{0.014}\right), \\ \lambda(M_t) &= 2(0.12711 + 0.00206(m_H - 125.66) - 0.00004(M_t - 173.10)).\end{aligned}\tag{4.20}$$

We employ  $m_W = 80.384$  (in GeV),  $\alpha_s = 0.1184$ ,  $M_t = 173.34$  (in GeV) from the combined measurements by the Tevatron and the LHC experiments [31], and  $m_H = 125.09$  (in GeV) from the combined analysis by the ATLAS and the CMS [4].

In Fig. 4.2, we show the RG running of the Higgs quartic coupling. The running Higgs quartic coupling is reducing towards high energies and eventually become negative. In the SM, this result is known as the electroweak vacuum instability problem. However, in our

GHU scenario, we interpret the scale at which  $\lambda(\mu) = 0$  as the compactification scale. In this figure, we find  $m_{KK} = 4.4 \times 10^9$  GeV.

When we assume only the SM particle contents below the compactification scale, the resultant  $m_{KK}$  is far above the electroweak scale. As we have found in equation 4.5, the Higgs self-energy is proportional to  $m_{KK}^2$ . So, if  $m_{KK}$  is much higher than the electroweak scale, we need a fine tuning to reproduce the correct Higgs VEV. The compactification scale at the TeV scale is desired to solve the gauge hierarchy problem. To lower the compactification scale, we need additional negative contribution to the beta function of the Higgs quartic coupling. It is clear from the formula of  $\beta_\lambda^{(1)}$  that new fermions with a sizable coupling with the Higgs doublet make the beta function more negative. For this purpose, in the following chapter, we introduce bulk fermions into our GHU model which provide KK modes lighter than the compactification scale.

## 5 HIGGS BOSON MASS WITH THE GAUGE-HIGGS CONDITION

We now investigate the way to reproduce the Higgs boson mass of around 125 GeV in this 5-dimensional GHU model. It is a highly non-trivial task to propose a realistic GHU scenario and calculate the Higgs boson mass in the context. However, in our effective theory approach, the Higgs boson mass is easily calculated from the RG evolution of the Higgs quartic coupling with the gauge-Higgs condition at the compactification scale, assuming the electroweak symmetry breaking is correctly achieved. In order to reproduce the 125 GeV Higgs boson mass for  $M_{\text{KK}} \ll 10^{10}$  GeV, we need to introduce a new fermion in the bulk. In this dissertation, we introduce color singlet/triplet, **6** and **10**-plet bulk fermions of the bulk  $SU(3)$  gauge symmetry with  $U(1)'$  charge  $Q$  as an example. We impose a (half) periodic boundary condition on the bulk fermions,  $\psi(y + 2\pi R) = \psi(y)$  ( $\psi(y + 2\pi R) = -\psi(y)$ ). To avoid massless states in the periodic bulk fermions, we introduce  $N_f$  pairs of the bulk fermion multiplets with opposite parities and a  $Z_2$ -parity even bulk mass term between each pair of the bulk fermions. In the same way, we introduce  $N_f^{\text{HP}}$  pairs of half-periodic fermions with the  $Z_2$ -parity even bulk mass term, when we consider half-periodic bulk fermions.

We begin with the **6**-plet of the bulk  $SU(3)$  gauge symmetry, which is decomposed into the representations under the  $SU(2) \times U(1)$  subgroup as

$$\mathbf{6} = \mathbf{1}_{-2/3} \oplus \mathbf{2}_{-1/6} \oplus \mathbf{3}_{1/3}, \quad (5.1)$$

where the numbers in the subscript denote the  $U(1)$  charges. For these multiplets, the bulk  $SU(3)$  gauge interaction leads to the Yukawa interaction of the form,

$$\mathcal{L} \supset -Y_S \bar{D}HS - Y_D \bar{D}TH^\dagger, \quad (5.2)$$

where  $S$ ,  $D$  and  $T$  stand for the singlet, doublet and triplet fields in the decomposition of Eq. (5.1), and  $Y_S$  and  $Y_D$  are Yukawa couplings. Because of the unification of the gauge

and Yukawa interactions,  $Y_S = Y_D = -ig_2$  at the compactification scale, where  $g_2$  is the SM SU(2) gauge coupling. In solving RG equations, this condition is also imposed as the boundary condition at the compactification scale. After the electroweak symmetry breaking the KK mass spectrum is found as follows:

$$\begin{aligned}
\left(m_{n,-2/3}^{(\pm)}\right)^2 &= (m_n \pm 2m_W)^2 + M^2, \quad m_n^2 + M^2, \\
\left(m_{n,+1/3}^{(\pm)}\right)^2 &= (m_n \pm m_W)^2 + M^2, \\
\left(m_{n,+4/3}^{(\pm)}\right)^2 &= m_n^2 + M^2,
\end{aligned} \tag{5.3}$$

where the numbers in the subscript denote the “electric charges”<sup>1</sup> of the corresponding KK mode fermions,  $m_n = nM_{\text{KK}}$  with  $n = 0, 1, 2, \dots$ ,  $M_{\text{KK}} \equiv 1/R_c$ ,  $m_W = g_2 v/2$  with  $v = 246$  GeV, and  $M$  is a bulk mass. For simplicity, we use a common bulk mass  $M$  for the  $N_f$  pairs. When a half periodic boundary condition is imposed on the bulk fermion, the KK mass spectrum are obtained by replacing  $n$  to  $n + 1/2$ .

In the same way, we decompose the **10**-plet as

$$\mathbf{10} = \mathbf{1}_{-1} \oplus \mathbf{2}_{-1/2} \oplus \mathbf{3}_0 \oplus \mathbf{4}_{1/2}. \tag{5.4}$$

For these multiplets, the bulk SU(3) gauge interaction leads to the Yukawa interaction of the form,

$$\mathcal{L} \supset -Y_S \bar{D}HS - Y_D \bar{D}TH^\dagger - Y_T \bar{F}TH, \tag{5.5}$$

where  $S$ ,  $D$ ,  $T$  and  $F$  stand for the singlet, doublet, triplet and quoted fields in the decomposition of Eq. (5.4), and  $Y_S$ ,  $Y_D$  and  $Y_T$  are Yukawa couplings. Because of the unification of the gauge and Yukawa interactions,  $Y_S = Y_T = -i\sqrt{3/2} g_2$  and  $Y_D = -i\sqrt{2} g_2$  at the compactification scale. These conditions are imposed as the boundary condition at the compactification scale in our RG analysis. The KK mass spectrum after the electroweak

---

<sup>1</sup>Here “electric charges” mean by electric charges of  $\text{SU}(2) \times \text{U}(1) \subset \text{SU}(3)$ . A true electric charge of each KK mode is given by a sum of the “electric charge” and U(1)’ charge  $Q$ .



symmetry breaking is found as

$$\begin{aligned}
\left(m_{n,-1}^{(\pm)}\right)^2 &= (m_n \pm 3m_W)^2 + M^2, & (m_n \pm m_W)^2 + M^2, \\
\left(m_{n,0}^{(\pm)}\right)^2 &= (m_n \pm 2m_W)^2 + M^2, & m_n^2 + M^2, \\
\left(m_{n,+1}^{(\pm)}\right)^2 &= (m_n \pm m_W)^2 + M^2, \\
\left(m_{n,+2}^{(\pm)}\right)^2 &= m_n^2 + M^2.
\end{aligned} \tag{5.6}$$

Although the  $U(1)'$  charge  $Q$  is a free parameter of the model, we have phenomenologically favored values for it from the following discussion. As discussed in [32] (see also [33, 34, 35, 36]), the lightest KK mode of a half-periodic bulk fermion, independently of the background metric, is stable in the effective 4-dimensional theory due to an accidental  $Z_2$  discrete symmetry. If the half-periodic bulk fermion is color-singlet, it is a good candidate for the cosmological dark matter. Even for the periodic bulk fermion, we are allowed to introduce an odd-parity while all the SM particles are even under the parity, in order to ensure the stability of the lightest KK mode. Thus, it is reasonable to assign the  $U(1)'$  charge  $Q$  to make the lightest KK mode electrically neutral. Since the electric charge is given by the sum of the charge of the  $U(1)$  subgroup in the bulk  $SU(3)$  and  $Q$ , we may choose  $Q = 2/3$  ( $Q = 1$ ) for a color-singlet, **6**-plet (**10**-plet) bulk fermion. However, a colored stable particle is cosmologically disfavored. For a color-triplet bulk fermion, we may introduce a mixing between the lightest colored KK fermion and a SM quark on the brane, so that the lightest KK fermion can decay to the SM quarks. There are two choices for the  $U(1)'$  charge to make the electric charge of the lightest KK mode to be  $-1/3$  or  $2/3$  for realizing a mixing with either the SM down-type quarks or up-type quarks. For the **6**-plet case, we may choose  $Q = 1/3$  or  $4/3$ , while  $Q = 2/3$  or  $5/3$  for the **10**-plet case.

Let us now analyze the RG equations. In our analysis, we neglect the KK mode mass splitting by the electroweak symmetry breaking and set the lightest fermion mass as  $m_0 = M$ . When we impose a half periodic boundary condition for the bulk fermions,

$$m_0 = \frac{1}{2}M_{\text{KK}}\sqrt{1 + 4c_B^2} \tag{5.7}$$

where  $c_B \equiv M/M_{\text{KK}}$ . For renormalization scale  $\mu < m_0$ , the bulk fermions are decoupled, and we employ the SM RG equations at the two-loop level [37], which were presented in chapter 4. For the renormalization scale  $\mu \geq m_0$ , the SM RG equations are modified in the presence of the bulk fermions. In this dissertation, we take only one-loop corrections from the bulk fermions into account. For the case with  $N_f$  pairs of **6**-plet periodic fermions (we identify  $N_f$  as  $N_f = 2N_f^{\text{HP}}$  for the case with  $N_f^{\text{HP}}$  pairs of half-periodic fermions), the beta functions of the SU(2) and U(1)<sub>Y</sub> gauge couplings receive new contributions as

$$\Delta b_1 = N_f N_c \left( \frac{2}{3} + \frac{24}{5} Q^2 \right), \quad \Delta b_2 = \frac{10}{3} N_f N_c, \quad \Delta b_3 = 4N_f \left( \frac{N_c - 1}{2} \right), \quad (5.8)$$

where  $N_c = 1$  ( $N_c = 3$ ) when the **6**-plet bulk fermions are color singlet (triplet). The beta functions of the top Yukawa and Higgs quartic couplings are modified as

$$\begin{aligned} \beta_t^{(1)} &\rightarrow \beta_t^{(1)} + y_t N_f N_c (2|Y_S|^2 + 3|Y_D|^2), \\ \beta_\lambda^{(1)} &\rightarrow \beta_\lambda^{(1)} + N_f N_c [\lambda (8|Y_S|^2 + 12|Y_D|^2) \\ &\quad - (8|Y_S|^4 + 10|Y_D|^4 + 16|Y_S|^2|Y_D|^2)], \end{aligned} \quad (5.9)$$

where the Yukawa couplings obey the following RG equations:

$$\begin{aligned} 16\pi^2 \frac{dY_S}{d \ln \mu} &= Y_S \left[ 3y_t^2 - \left( \frac{9}{20}g_1^2 + \frac{9}{4}g_2^2 \right) + N_f \left( \frac{4N_c + 3}{2}|Y_S|^2 + \frac{12N_c + 7}{4}|Y_D|^2 \right) \right. \\ &\quad \left. - (N_c^2 - 1)g_3^2 - \frac{18}{5} \left( \frac{2}{3} - Q \right) \left( \frac{1}{6} - Q \right) g_1^2 \right], \\ 16\pi^2 \frac{dY_D}{d \ln \mu} &= Y_D \left[ 3y_t^2 - \left( \frac{9}{20}g_1^2 + \frac{9}{4}g_2^2 \right) + N_f \left( \frac{4N_c + 5}{2}|Y_S|^2 + \frac{12N_c + 5}{4}|Y_D|^2 \right) \right. \\ &\quad \left. - (N_c^2 - 1)g_3^2 - 6g_2^2 - \frac{18}{5} \left( \frac{1}{6} - Q \right) \left( \frac{1}{3} - Q \right) g_1^2 \right]. \end{aligned} \quad (5.10)$$

In our RG analysis, we numerically solve the RG equations with the bulk fermions from  $M_{\text{KK}}$  to  $m_0$  for a fixed  $M_{\text{KK}}$  by imposing the gauge-Higgs condition and the unification condition between the gauge and Yukawa couplings such that

$$\lambda(M_{\text{KK}}) = 0, \quad Y_S(M_{\text{KK}}) = Y_D(M_{\text{KK}}) = -ig_2(M_{\text{KK}}). \quad (5.11)$$

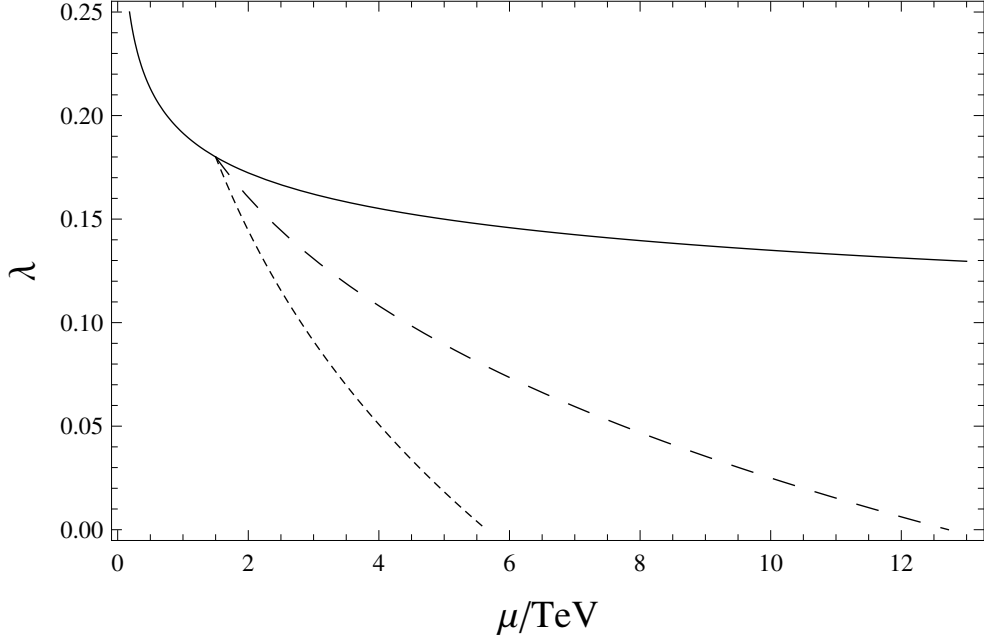


Fig. 5.1.: The RG evolutions of the Higgs quartic coupling, which can reproduce the Higgs boson pole mass  $m_H = 125.09$  GeV. The solid line denotes the running Higgs quartic coupling in the SM. The dashed and dotted lines correspond, respectively, to the **6**-plets for  $N_f = 2$ ,  $N_c = 1$ ,  $Q = 2/3$  and  $(M_{\text{KK}}, m_0) = (12.7, 1.5)$  TeV, and the **6**-plet for  $N_f = 2$ ,  $N_c = 3$ ,  $Q = 4/3$  and  $(M_{\text{KK}}, m_0) = (5.65, 1.5)$  TeV.

For the renormalization scale  $\mu < m_0$ , we obtain numerical solutions to the SM RG equations. The lightest fermion mass  $m_0$  is a free parameter, which is determined so as to smoothly connect the running Higgs quartic couplings in two regions,  $\mu < m_0$  and  $\mu > m_0$ , at  $m_0$ .

The running Higgs quartic coupling to reproduce the Higgs boson pole mass  $m_H = 125.09$  GeV is shown in Fig. 5.1. The solid line denotes the running quartic coupling in the SM, while the dashed (dotted) line corresponds to the result for the case with  $N_f = 1$  ( $N_f = 2$ ) pair of **6**-plet, color singlet (triplet) bulk fermions with  $U(1)'$  charge  $Q = 2/3$  ( $Q = 4/3$ ). For the dashed (dotted) line, we find  $m_0 = 1.5$  TeV for  $M_{\text{KK}} = 5.65$  (12.7) TeV, at which the gauge-Higgs condition is satisfied. When we trace the dashed and dotted lines from  $M_t$  to higher energies we see that the running of the Higgs quartic coupling is drastically altered from the SM one (solid line) due to the contributions from the bulk fermions with  $m_0 = 1.5$  TeV. Since the beta function of the Higgs quartic coupling becomes more negative in the presence of the bulk fermions (see Eq. (5.9)), the running Higgs quartic coupling reaches the

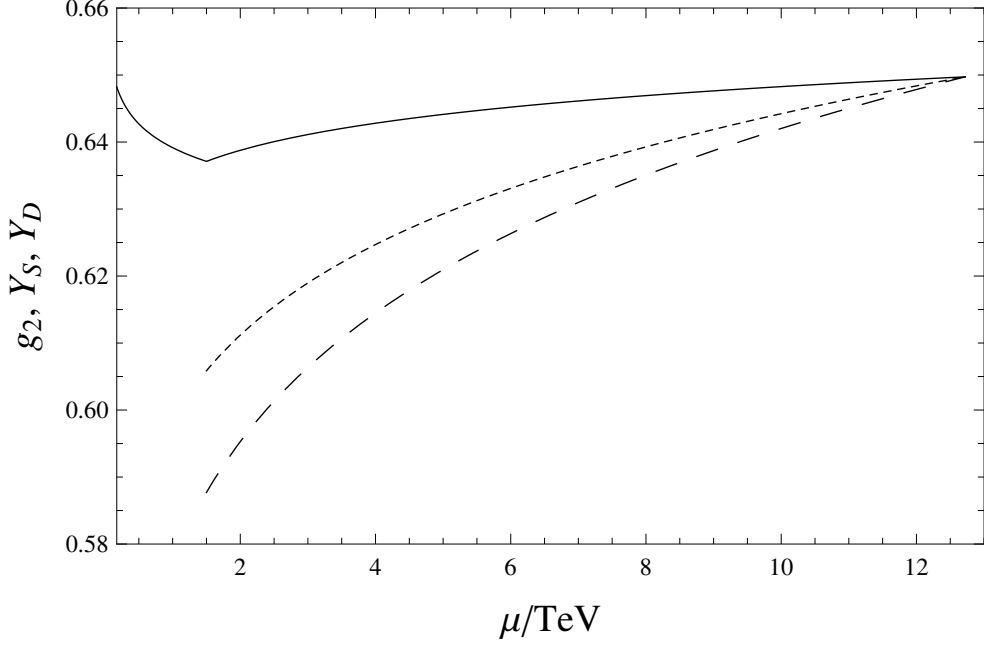


Fig. 5.2.: The RG evolutions of the SM SU(2) gauge coupling (solid line) and Yukawa couplings  $|Y_S|$  (dashed line) and  $|Y_D|$  (dotted line) for the case with  $N_f = 1$  pair of **6**-plet, color singlet bulk fermions. We can see that the boundary condition from the unification among the gauge and Yukawa couplings,  $|Y_S| = |Y_D| = g_2$ , is satisfied at  $M_{\text{KK}} = 12.7$  TeV.

compactification scale far below  $10^{10}$  GeV. We also show in Fig. 5.2 the RG evolutions of the SM SU(2) gauge coupling (solid line) and Yukawa couplings  $|Y_S|$  (dashed line) and  $|Y_D|$  (dotted line) for the case with  $N_f = 1$  pair of **6**-plet, color singlet bulk fermions. We can see that the boundary condition from the unification between the gauge and Yukawa couplings,  $|Y_S| = |Y_D| = g_2$ , is satisfied at  $M_{\text{KK}} = 12.7$  TeV.

Once the compactification scale  $M_{\text{KK}}$  is fixed, the lightest fermion mass  $m_0$  is determined so as to reproduce the Higgs boson pole mass  $m_H = 125.09$  GeV. The relation between  $m_0$  and  $M_{\text{KK}}$  is depicted in Fig. 5.3. In the top panel we show the relation for the color singlet, **6**-plet bulk fermions with  $N_f = 1$  (solid line) and  $N_f = 2$  (dashed line). Here we have taken  $Q = 2/3$  as an example. The relations for the color triplet, **6**-plet bulk fermions with  $N_f = 1$  (solid line) and  $N_f = 2$  (dashed line), respectively, are shown in the bottom panel. For the color triplet case, we have taken  $Q = 4/3$ . As the number of bulk fermions is increasing, the compactification scale for a fixed  $m_0$  is decreasing.

For the color singlet, **6**-plet bulk fermions with  $N_f = 1$ , we show in Fig. 5.4 the relation

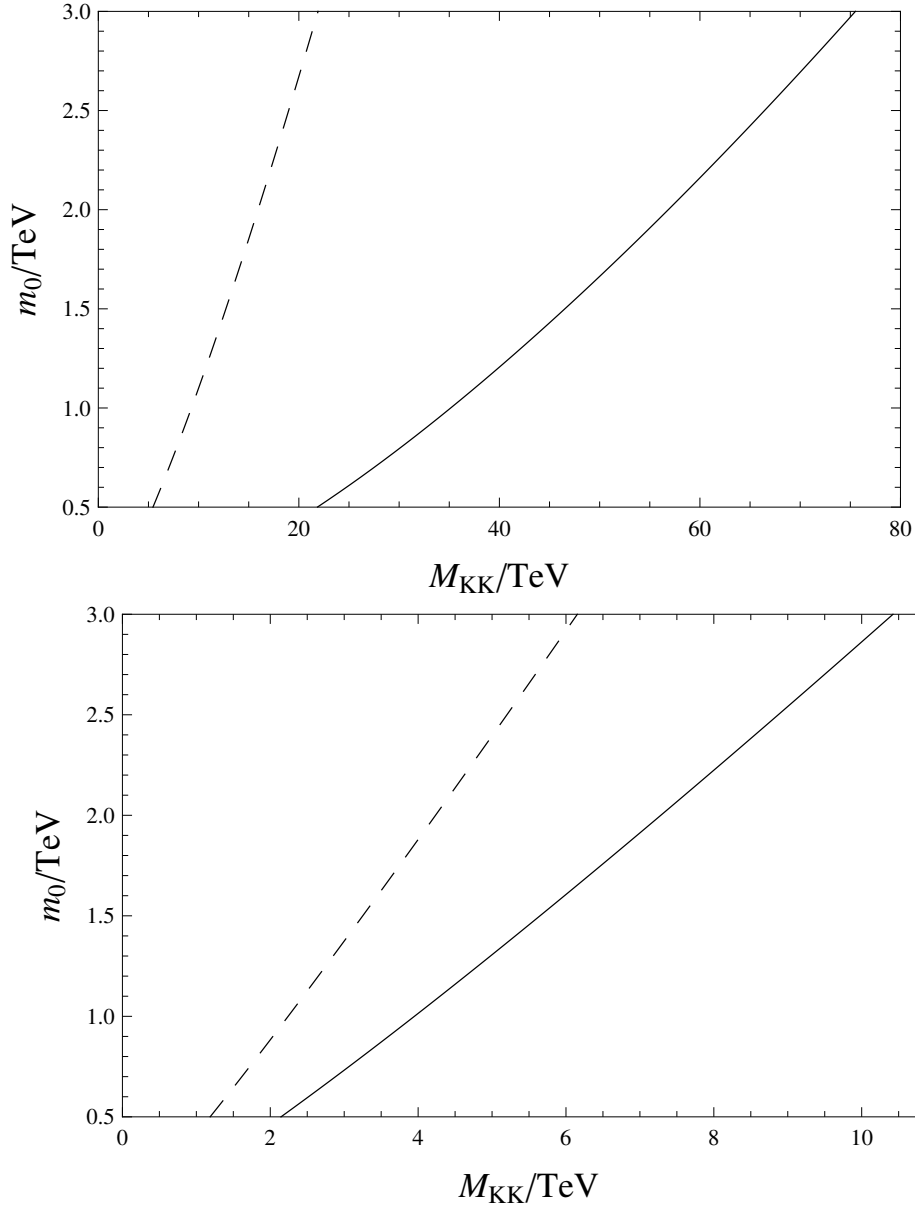


Fig. 5.3.: The relation between  $M_{\text{KK}}$  and  $m_0$  to reproduce the Higgs boson pole mass  $m_H = 125.09$  GeV. The top panel shows the results for the color singlet, **6**-plet bulk fermions with  $N_f = 1$  (solid line) and  $N_f = 2$  (dashed line). Here we have taken  $Q = 2/3$ . The bottom panel shows the results for the color triplet, **6**-plet bulk fermions with  $N_f = 1$  (solid line) and  $N_f = 2$  (dashed line). For the color triplet case, we have taken  $Q = 4/3$ .

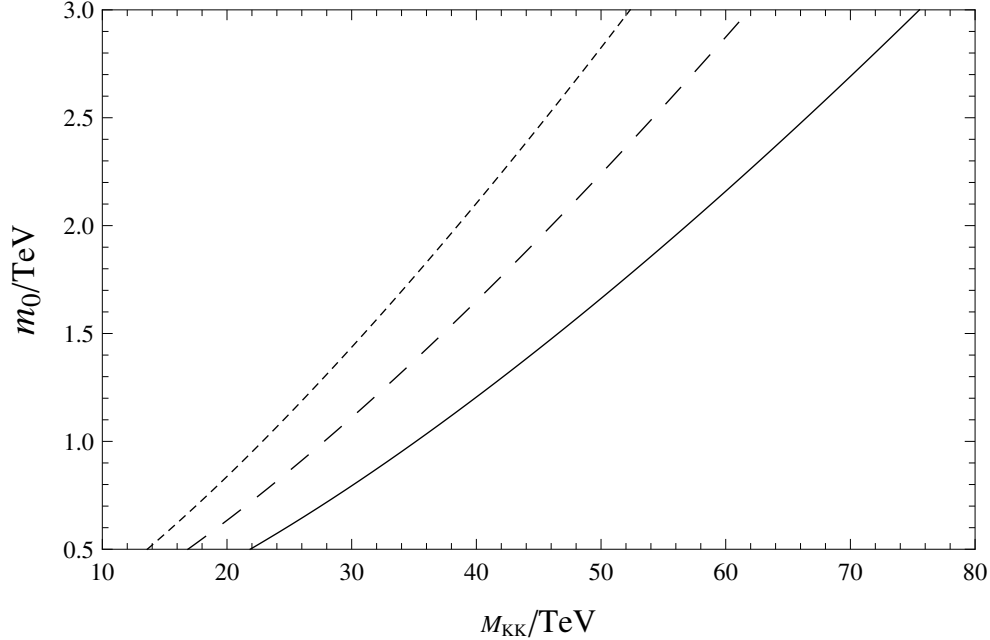


Fig. 5.4.: The relation between  $M_{\text{KK}}$  and  $m_0$  to reproduce the Higgs boson pole mass  $m_H = 125.09$  GeV for various  $U(1)'$  charges. The solid, dashed and dotted lines corresponds to the results for  $Q = 0, 2$  and  $-2$ , respectively.

between  $M_{\text{KK}}$  and  $m_0$  for various  $U(1)'$  charges. The solid, dashed and dotted lines corresponds to the results for  $Q = 0, 2$  and  $-2$ , respectively. We find that the compactification scale for a fixed  $m_0$  is decreasing, as  $|Q|$  is increasing.

We perform the same analysis for the case with the  $N_f$  pairs of the **10**-plet periodic fermions (we identify  $N_f$  as  $N_f = 2N_f^{\text{HP}}$  for the case with  $N_f^{\text{HP}}$  pairs of half-periodic fermions). For the renormalization scale  $\mu \geq m_0$ , the beta functions of the  $SU(2)$  and  $U(1)_Y$  gauge couplings receive new contributions as

$$\Delta b_1 = N_f N_c (3 + 12Q^2), \quad \Delta b_2 = 10N_f N_c, \quad \Delta b_3 = \frac{10}{3} N_f \left( \frac{N_c - 1}{2} \right), \quad (5.12)$$

where  $N_c = 1$  ( $N_c = 3$ ) when the **10**-plet bulk fermions are color singlet (triplet). The beta

functions of the top Yukawa and Higgs quartic couplings are modified as

$$\begin{aligned}
\beta_t^{(1)} &\rightarrow \beta_t^{(1)} + y_t N_f N_c (2|Y_S|^2 + 3|Y_D|^2), \\
\beta_\lambda^{(1)} &\rightarrow \beta_\lambda^{(1)} + N_f N_c (4\lambda (2|Y_S|^2 + 3|Y_D|^2 + 4|Y_T|^2)) \\
&\quad - N_f N_c \left( 8|Y_S|^4 + 10|Y_D|^4 + \frac{112}{9}|Y_T|^4 \right) \\
&\quad + N_f N_c \left( 16|Y_S|^2|Y_D|^2 + \frac{64}{3}|Y_D|^2|Y_T|^2 \right), \tag{5.13}
\end{aligned}$$

where the Yukawa couplings obey the following RG equations:

$$\begin{aligned}
16\pi^2 \frac{dY_S}{d\ln\mu} &= Y_S \left[ 3y_t^2 - \left( \frac{9}{20}g_1^2 + \frac{9}{4}g_2^2 \right) + N_f \left( \frac{4N_c + 3}{2}|Y_S|^2 + \frac{12N_c + 15}{4}|Y_D|^2 \right. \right. \\
&\quad \left. \left. + 4N_c|Y_T|^2 \right) - (N_c^2 - 1)g_3^2 - \frac{18}{5}(1 - Q) \left( \frac{1}{2} - Q \right) g_1^2 \right], \\
16\pi^2 \frac{dY_D}{d\ln\mu} &= Y_D \left[ 3y_t^2 - \left( \frac{9}{20}g_1^2 + \frac{9}{4}g_2^2 \right) + N_f \left( \frac{4N_c + 5}{2}|Y_S|^2 + \frac{12N_c + 5}{4}|Y_D|^2 \right. \right. \\
&\quad \left. \left. + \frac{12N_c + 10}{3}|Y_T|^2 \right) - (N_c^2 - 1)g_3^2 - 6g_2^2 - \frac{18}{5} \left( Q - \frac{1}{2} \right) Q g_1^2 \right], \\
16\pi^2 \frac{dY_T}{d\ln\mu} &= Y_T \left[ 3y_t^2 - \left( \frac{9}{20}g_1^2 + \frac{9}{4}g_2^2 \right) + N_f \left( 2N_c|Y_S|^2 + \frac{6N_c + 5}{2}|Y_D|^2 \right. \right. \\
&\quad \left. \left. + \frac{24N_c + 7}{6}|Y_T|^2 \right) (N_c^2 - 1)g_3^2 - 15g_2^2 - \frac{18}{5}Q \left( Q + \frac{1}{2} \right) g_1^2 \right]. \tag{5.14}
\end{aligned}$$

We numerically solve the RG equations with the bulk fermions from  $M_{\text{KK}}$  to  $m_0$  for a fixed  $M_{\text{KK}}$  by imposing the gauge-Higgs condition and the unification condition among the gauge and Yukawa couplings such that

$$\lambda(M_{\text{KK}}) = 0, \quad \sqrt{\frac{2}{3}}Y_S(M_{\text{KK}}) = \sqrt{\frac{1}{2}}Y_D(M_{\text{KK}}) = \sqrt{\frac{2}{3}}Y_T(M_{\text{KK}}) = -ig_2(M_{\text{KK}}). \tag{5.15}$$

For the renormalization scale  $\mu < m_0$ , we obtain numerical solutions to the SM RG equations. The lightest fermion mass  $m_0$  is determined so as to smoothly connect the running Higgs quartic couplings in two regions,  $\mu < m_0$  and  $\mu > m_0$ , at  $m_0$ , and hence to reproduce the Higgs boson pole mass of  $m_H = 125.09$  GeV. In Fig. 5.5, we show the relation between  $M_{\text{KK}}$  and  $m_0$ . The solid and dashed lines denotes the results for the color singlet, **10**-plet bulk

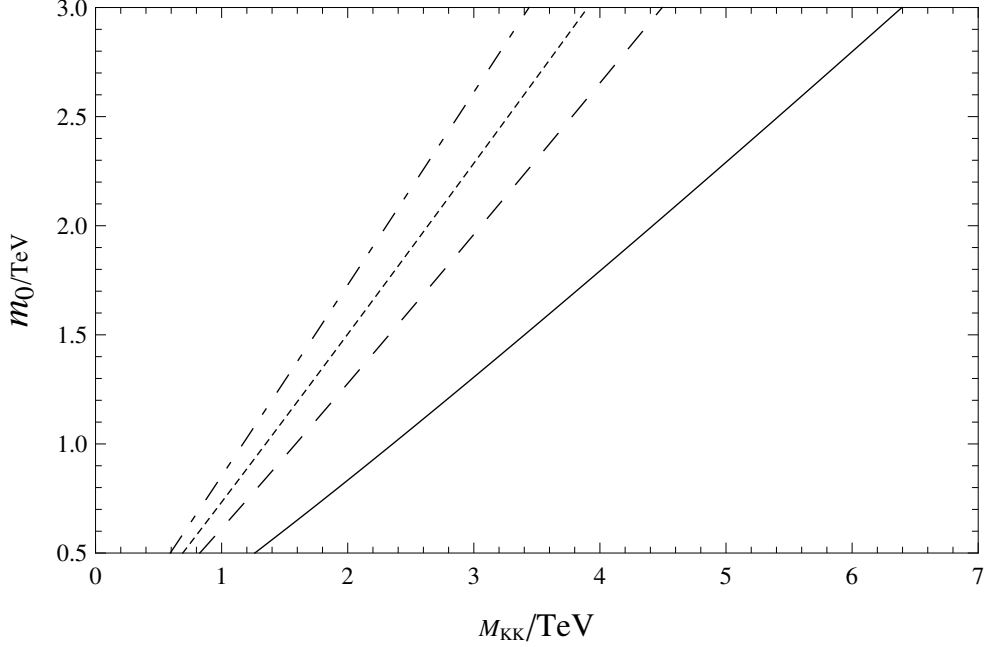


Fig. 5.5.: The relation between  $M_{\text{KK}}$  and  $m_0$  to reproduce the Higgs boson pole mass of  $m_H = 125.09$  GeV. The solid and dashed lines denote the results for the color singlet, **10**-plet bulk fermions with  $N_f = 1$  and  $N_f = 2$ , respectively. Here we have taken  $Q = 1$ . The dotted and dash-dotted lines represent the results for the color triplet, **10**-plet bulk fermions with  $N_f = 1$  and  $N_f = 2$  ( $N_f^{\text{HP}} = 1$ ), respectively. We have taken  $Q = 5/3$  for the **10**-plets.

fermions with  $N_f = 1$  and  $N_f = 2$ , respectively. Here we have taken  $Q = 1$ . The dotted and dash-dotted lines represent the results for the color triplet, **10**-plet bulk fermions with  $N_f = 1$  and  $N_f = 2$ , respectively. We have taken  $Q = 5/3$  for the **10**-plets. Note that along the dash-dotted line the relation of  $m_0 \geq M_{\text{KK}}/2$  is satisfied, and we can also consider a half-periodic boundary condition for this case with  $N_f^{\text{HP}} = 1$ .



## 6 HIGGS BOSON PRODUCTION AND DECAY IN GHU MODEL

Through quantum corrections at the one-loop level, the bulk fermions contribute to the Higgs boson production and decay processes and deviate the Higgs boson signal strengths at the LHC experiments from the SM predictions. In this section, we evaluate the contributions from the bulk **6**-plet and **10**-plet fermions to the Higgs boson production and decay processes at the LHC, and lead to a lower mass bound for the lightest bulk fermion.

### 6.1 Bulk Fermion Contributions to the Gluon Fusion Channel

At the LHC, the Higgs boson is dominantly produced via gluon fusion process with the following dimension five operator between the Higgs boson and di-gluon:

$$\mathcal{L}_{\text{eff}} = C_{gg} h G_{\mu\nu}^a G^{a\mu\nu} \quad (6.1)$$

where  $h$  is the SM Higgs boson, and  $G_{\mu\nu}^a$  ( $a = 1 - 8$ ) is the gluon field strength. The SM contribution to  $C_{gg}$  is dominated by top quark 1-loop corrections. As a good approximation, we express this contribution by using the Higgs low energy theorem [38],

$$C_{gg}^{\text{SMtop}} \simeq \frac{g_3^2}{32\pi^2 v} b_3^t \frac{\partial}{\partial \log v} \log M_t = \frac{\alpha_s}{12\pi v} \quad (6.2)$$

where  $\alpha_s = g_3^2/(4\pi)$ , and  $b_3^t = 2/3$  is a top quark contribution to the beta function coefficient of QCD.

In addition to the SM contribution, we take into account the contributions from the top quark KK modes. One might think that the KK mode contributions from the light SM fermions should be taken into account. However, they can be safely neglected compared to those from the top quark KK modes, since the effective coupling of the Higgs boson to di-gluon is generated by the electroweak symmetry breaking and hence proportional to the corresponding SM fermion masses. Thus, we only consider the top quark KK mode

contribution. In GHU scenario, we expect the top quark KK mode spectrum to be

$$m_{n,t}^{(\pm)} = m_n \pm M_t \quad (6.3)$$

where  $m_n \equiv nM_{\text{KK}}$  with an integer  $n = 1, 2, 3, \dots$ . Using the Higgs low energy theorem, we obtain

$$\begin{aligned} C_{gg}^{\text{KKtop}} &\simeq \frac{\alpha_s}{12\pi v} \sum_{n=1}^{\infty} \frac{\partial}{\partial \log v} [\log(m_n + M_t) + \log(m_n - M_t)] \\ &\simeq -\frac{\alpha_s}{6\pi v} \sum_{n=1}^{\infty} \left(\frac{M_t}{m_n}\right)^2 = -\frac{\alpha_s}{12\pi v} \times \frac{\pi^2}{3} \left(\frac{M_t}{M_{\text{KK}}}\right)^2, \end{aligned} \quad (6.4)$$

where we have used an approximation of  $M_t^2 \ll m_n^2$ , and  $\sum_{n=1}^{\infty} 1/n^2 = \pi^2/6$ . As pointed out in [21], the KK mode contribution to the effective Higgs coupling to di-gluon is destructive to the SM one.

The  $N_f$  pairs of color triplet, **6**-plet and **10**-plet bulk fermions have the KK mass spectra as shown in Eqs. (5.3) and (5.6), respectively. Applying the Higgs low energy theorem, their contributions to the Higgs-to-digluon coupling are calculated as

$$C_{gg}^{\text{KK6}} \simeq F(2m_W) + F(m_W), \quad (6.5)$$

$$C_{gg}^{\text{KK10}} \simeq F(3m_W) + F(2m_W) + 2F(m_W), \quad (6.6)$$

where the function  $F(m_W)$  is given by

$$\begin{aligned} F(m_W) &= 2N_f \frac{\alpha_s}{12\pi v} \sum_{n=-\infty}^{\infty} \frac{\partial}{\partial \log v} \left[ \log \sqrt{(m_n + m_W)^2 + M^2} \right] \\ &\simeq 2N_f \frac{\alpha_s}{12\pi v} \left(\frac{m_W}{M_{\text{KK}}}\right)^2 \left[ \frac{1}{c_B^2 + (m_W/M_{\text{KK}})^2} - 2 \sum_{n=1}^{\infty} \frac{n^2 - c_B^2}{(n^2 + c_B^2)^2} \right] \\ &= 2N_f \frac{\alpha_s}{12\pi v} \left(\frac{m_W}{M_{\text{KK}}}\right)^2 \left[ \frac{1}{c_B^2 + (m_W/M_{\text{KK}})^2} - \frac{1 - (\pi c_B / \sinh[\pi c_B])^2}{c_B^2} \right], \end{aligned} \quad (6.7)$$

for the bulk fermion for which a periodic boundary condition is imposed. When we impose

a half-periodic boundary condition, we have [8]

$$\begin{aligned}
F(m_W) &= 2N_f^{\text{HP}} \frac{\alpha_s}{12\pi v} \sum_{n=-\infty}^{\infty} \frac{\partial}{\partial \log v} \left[ \log \sqrt{M^2 + (m_{n+\frac{1}{2}} + m_W)^2} \right] \\
&\simeq -2N_f^{\text{HP}} \frac{\alpha_s}{6\pi v} \left( \frac{m_W}{M_{\text{KK}}} \right)^2 \sum_{n=0}^{\infty} \frac{(n + \frac{1}{2})^2 - c_B^2}{\left( (n + \frac{1}{2})^2 + c_B^2 \right)^2} \\
&= -2N_f^{\text{HP}} \frac{\alpha_s}{12\pi v} \left( \frac{m_W}{M_{\text{KK}}} \right)^2 \frac{\pi^2}{\cosh^2[\pi c_B]}.
\end{aligned} \tag{6.8}$$

Here,  $c_B = M/M_{\text{KK}}$ , and we have used the approximation  $m_W^2 \ll M_{\text{KK}}^2$ .

Now we evaluate the ratio of the Higgs production cross section through the gluon fusion at the LHC to the SM one as

$$R_{gg} \equiv \left( 1 + \frac{C_{gg}^{\text{KKtop}} + C_{gg}^{\text{KK6/10}}}{C_{gg}^{\text{SMtop}}} \right)^2. \tag{6.9}$$

In the previous section, we have found a relation between  $M_{\text{KK}}$  and  $m_0$  for the color triplet bulk fermions to reproduce the Higgs boson pole mass of  $m_H = 125.09$  GeV (see Figs. 5.3 and 5.5). With the relation, we can express the ratio  $R_{gg}$  as a function of  $m_0$ . Our results are shown in Fig. 6.1. The top panel shows the ratio in the presence of the color-triplet, bulk **6**-plet fermions for which the relation between  $M_{\text{KK}}$  and  $m_0$  are shown in the bottom panel of Fig. 5.3. The solid and dashed lines in the top panel of Fig. 6.1 correspond to the solid and dashed lines in the bottom panel of Fig. 5.3. The bottom panel of Fig. 6.1 shows the results for the color-triplet, **10**-plet bulk fermions with  $N_f = 1$  and  $Q = 5/3$ . The relation between  $M_{\text{KK}}$  and  $m_0$  for the fermions is shown as the dotted and dash-dotted line in Fig. 5.5. Note that this relation along the dashed-dotted line satisfies  $m_0 \geq M_{\text{KK}}/2$ , so that we can also apply to a half-periodic boundary condition for the **10**-plet fermions with  $N_f^{\text{HP}} = 1$ . Here we have considered the periodic boundary condition for the dotted line in Fig. 5.5, while the half-periodic boundary condition for the dash-dotted line in Fig. 5.5. The dotted and dash-dotted lines represent the results for the periodic and half-periodic **10**-plet fermions, respectively.

In the presence of the bulk fermions, the Higgs production cross section in the gluon

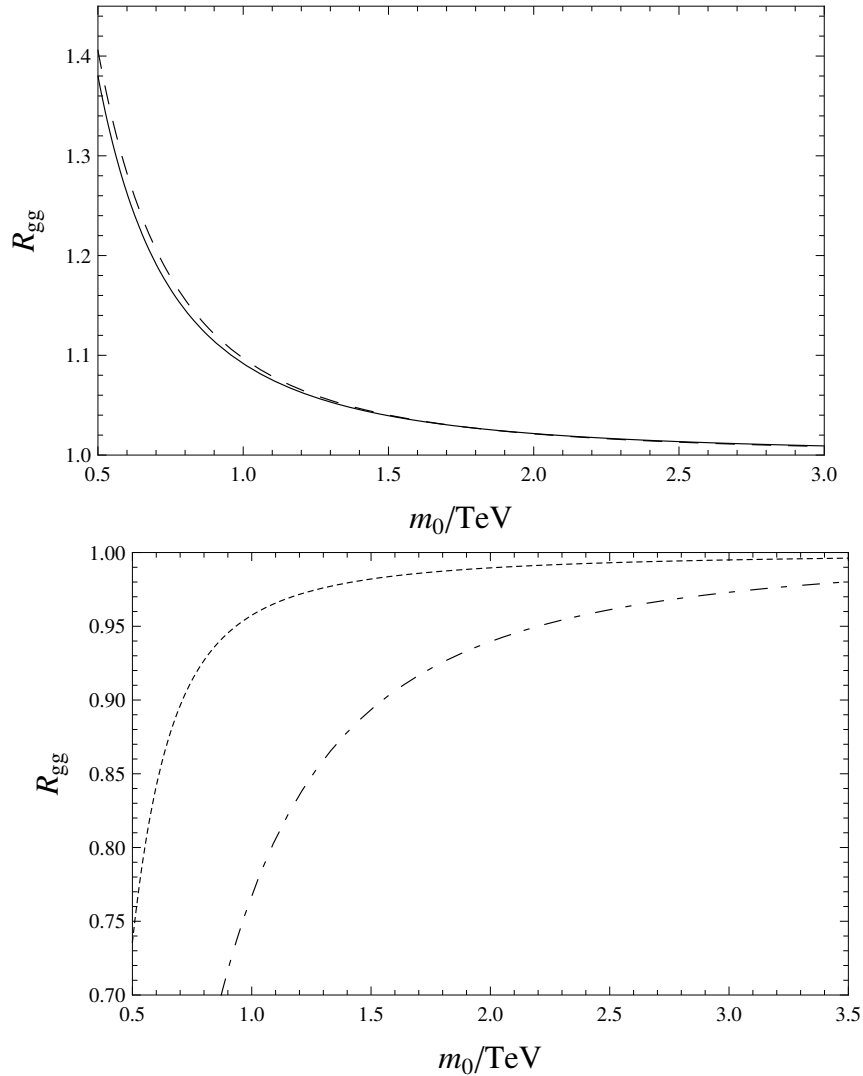


Fig. 6.1.: The ratio of the Higgs production cross section in our model to the SM one as a function of the lightest bulk fermion mass  $m_0$ . The top panel shows the results for the **6**-plet case corresponding to the bottom panel of Fig. 5.3. The results for the **10**-plet case, corresponding to the dotted and dash-dotted lines in Fig. 5.5, are depicted in the right panel. Here we have considered the periodic boundary condition for the dotted line in Fig. 5.5, while the half-periodic boundary condition for the dash-dotted line Fig. 5.5. The dotted and dash-dotted lines represent the results for the periodic and half-periodic **10**-plet fermions, respectively.

fusion channel is altered from the SM prediction. This deviation becomes larger as  $m_0$  (or equivalently,  $M_{\text{KK}}$ ) is lowered. Since the Higgs boson properties measured by the LHC experiments are found to be consistent with the SM predictions [5], we can find a lower bound for  $m_0$  from the LHC results. Employing the results from a combined analysis by the ATLAS and the CMS collaborations [5],  $0.88 \leq R_{gg} \leq 1.2$ , we can read off a lower bound of the lightest bulk fermion mass  $m_0$  from Fig. 6.1. Our results are summarized in Table 6.1. The lower bounds are found to be at TeV, so that such exotic colored particles can be tested at the LHC Run II with  $\sqrt{s} = 13 - 14$  TeV.

	BC	$N_f^{\text{HP}}$	$Q$	$m_0$ (TeV)	$M_{\text{KK}}$ (TeV)
<b>6</b> -plet	P	1	4/3	0.685	2.83
<b>6</b> -plet	P	2	4/3	0.710	1.64
<b>10</b> -plet	P	1	5/3	0.663	0.908
<b>10</b> -plet	HP	1	5/3	1.41	1.64
top quark KK mode					1.26

Table 6.1.: The lower bound on the lightest bulk fermion masses and the compactification scales from the ATLAS and CMS combined analysis,  $0.88 \leq R_{gg} \leq 1.2$ , for the cases with the color-triplet, **6** or **10**-plet bulk fermion. Here, the initials, “BC”, “P” and “HP” stand for “boundary condition”, “periodic” and “half-periodic”, respectively. We have also shown in the last row the lower bound on the compactification scale when only the top quark KK modes is taken into account.

## 6.2 Bulk fermion contributions to $h \rightarrow \gamma\gamma$

Since the bulk fermions have electric charges, they also contribute to the effective Higgs boson coupling with di-photon of the dimension five operator,

$$\mathcal{L}_{\text{eff}} = C_{\gamma\gamma} h F_{\mu\nu} F^{\mu\nu}, \quad (6.10)$$

where  $F_{\mu\nu}$  denotes the photon field strength. In the SM, this effective coupling is induced by the top quark and  $W$ -boson loop corrections. In addition to the SM contributions, we have contributions from the KK modes of top quark,  $W$ -boson, and the **6**-plet and **10**-plet bulk fermions.

We begin with the top quark loop contribution. By using the Higgs low energy theorem,

we have

$$C_{\gamma\gamma}^{\text{SMtop}} \simeq \frac{e^2 b_1^t}{32\pi^2 v} \frac{\partial}{\partial \log v} \log m_t = \frac{2\alpha_{em}}{9\pi v}, \quad (6.11)$$

where  $b_1 = (4/3) \times (2/3)^2 \times 3 = 4/3$  is a top quark contribution to the QED beta function coefficient, and  $\alpha_{em}$  is the fine structure constant. Corresponding KK top quark contribution is given by

$$\begin{aligned} C_{\gamma\gamma}^{\text{KKtop}} &\simeq \frac{e^2 b_1^t}{32\pi^2 v} \sum_{n=1}^{\infty} \frac{\partial}{\partial \log v} [\log(m_n + M_t) + \log(m_n - M_t)] \\ &\simeq -\frac{2\alpha_{em}}{9\pi v} \times \frac{\pi^2}{3} \left( \frac{M_t}{M_{\text{KK}}} \right)^2. \end{aligned} \quad (6.12)$$

As the same for the contribution to the effective Higgs coupling with digluon, the KK top quark contribution is destructive to the top quark contribution.

Applying the Higgs low energy theorem, the SM  $W$ -boson loop contribution is calculated as

$$C_{\gamma\gamma}^W \simeq \frac{e^2}{32\pi^2 v} b_1^W \frac{\partial}{\partial \log v} \log m_W = -\frac{7\alpha_{em}}{8\pi v} \quad (6.13)$$

where  $m_W = g_2 v/2$ , and  $b_1^W = -7$  is a  $W$ -boson contribution to the QED beta function coefficient. Since  $4m_W^2/m_h^2 \gg 1$  is not well satisfied, this estimate is rough. In the following numerical analysis, we use the known loop-functions for the  $W$ -boson loop correction [38].

In our model, the KK mode mass spectrum of the  $W$ -boson is given by

$$m_{n,W}^{(\pm)} = m_n \pm m_W, \quad (6.14)$$

so that the contribution from KK  $W$ -boson loop diagrams is found to be

$$\begin{aligned} C_{\gamma\gamma}^{\text{KKW}} &= \frac{e^2}{32\pi^2 v} b_1^W \sum_{n=1}^{\infty} \frac{\partial}{\partial \log v} [\log(m_n + m_W) + \log(m_n - m_W)] \\ &\simeq \frac{7\alpha_{em}}{8\pi v} \frac{\pi^2}{3} \left( \frac{m_W}{M_{\text{KK}}} \right)^2. \end{aligned} \quad (6.15)$$

Note again that the KK  $W$ -boson contribution is destructive to the SM  $W$ -boson contribution.

Finally, the **6**-plet or **10**-plet loop contributions can be read from the KK-mode mass spectrum in Eq. (5.3) or (5.6) and the electric charges of each modes:

$$C_{\gamma\gamma}^{\text{KK6}} \simeq \left(Q - \frac{2}{3}\right)^2 \hat{F}(2m_W) + \left(Q + \frac{1}{3}\right)^2 \hat{F}(m_W) \quad (6.16)$$

$$C_{\gamma\gamma}^{\text{KK10}} \simeq (Q - 1)^2 \hat{F}(3m_W) + (Q - 1)^2 \hat{F}(m_W) + Q^2 \hat{F}(2m_W) + (Q + 1)^2 \hat{F}(m_W), \quad (6.17)$$

where  $Q$  is a  $U(1)'$  charge for the **6** and **10**-plets, and

$$\hat{F}(m_W) \simeq 2N_f N_c \frac{\alpha_{em}}{6\pi v} \left(\frac{m_W}{M_{\text{KK}}}\right)^2 \left[ \frac{1}{c_B^2 + (m_W/M_{\text{KK}})^2} - \frac{1 - (\pi c_B / \sinh[\pi c_B])^2}{c_B^2} \right], \quad (6.18)$$

for the periodic bulk fermions, while for the half-periodic bulk fermions, we have

$$\hat{F}(m_W) \simeq -2N_f^{\text{HP}} N_c \frac{\alpha_{em}}{6\pi v} \left(\frac{m_W}{M_{\text{KK}}}\right)^2 \frac{\pi^2}{\cosh^2[\pi c_B]}. \quad (6.19)$$

Here, we have used the approximation  $m_W^2 \ll M_{\text{KK}}^2$ .

The ratio of the partial decay width of  $h \rightarrow \gamma\gamma$  in our model to the SM one is given by

$$R_{\gamma\gamma} = \left( 1 + \frac{C_{\gamma\gamma}^{\text{KKtop}} + C_{\gamma\gamma}^{\text{KKW}} + C_{\gamma\gamma}^{\text{KK6/10}}}{C_{\gamma\gamma}^{\text{SMtop}} + C_{\gamma\gamma}^{\text{W}}} \right)^2. \quad (6.20)$$

If the bulk fermions are color-singlet, they have no effect on the Higgs boson production cross section. In this case, the effect of the bulk fermions can be seen in a deviation of the signal strength of the Higgs diphoton decay mode. Since the branching fraction of  $h \rightarrow \gamma\gamma$  is of order 0.1%, the deviation of the signal strength from the SM prediction is evaluated by  $R_{\gamma\gamma}$ . The relation between  $m_0$  and  $M_{\text{KK}}$  is determined so as to reproduce  $m_H = 125.09$  GeV, we evaluate  $R_{\gamma\gamma}$  as a function of  $m_0$  for the color-singlet, **6**-plet and **10**-plet bulk fermions. Our results are shown in Fig. 6.2. The top panel shows the results for the **6**-plet case presented

in the top panel of Fig. 5.3. The solid and dashed lines are corresponding to the same types of lines in the top panel of Fig. 5.3. The results for the **10**-plet case, which correspond to the solid and dashed lines in Fig. 5.5, are depicted in the bottom panel.

To derive a lower bound on  $m_0$ , we employ the results of the signal strength from a combined analysis by the ATLAS and the CMS collaborations [5] such as  $0.98 \leq \mu^{\gamma\gamma} \leq 1.36$ , which is identified as  $R_{\gamma\gamma}$  in our case. We then read off a lower bound on the lightest bulk fermion mass  $m_0$  from Fig. 6.2. Our results are summarized in Table 6.2.

	BC	$N_f$	$Q$	$m_0$ (TeV)	$M_{\text{KK}}$ (TeV)
<b>6</b> -plet	P	1	2/3	0.507	22.1
<b>6</b> -plet	P	2	2/3	0.719	28.0
<b>10</b> -plet	P	1	1	1.05	2.46
<b>10</b> -plet	P	2	1	2.10	3.20

Table 6.2.: The lower bound on the lightest bulk fermion masses and the compactification scales from the ATLAS and CMS combined analysis,  $0.98 \leq \mu^{\gamma\gamma} \simeq R_{\gamma\gamma} \leq 1.36$ , for the cases with the color-singlet, **6** and **10**-plet bulk fermions.

	BC	$N_f^{\text{HP}}$	$Q$	$m_0$ (TeV)	$M_{\text{KK}}$ (TeV)
<b>10</b> -plet	P	1	5/3	2.30	3.01
<b>10</b> -plet	HP	1	5/3	2.46	2.83

Table 6.3.: The lower bound on the lightest bulk colored fermion masses and the compactification scales from the ATLAS and CMS combined analysis,  $0.98 \leq \mu^{\gamma\gamma} \leq 1.36$ . We have obtained the lower bound only for the **10**-plet bulk fermions.

### 6.3 Bulk colored fermion contributions to $gg \rightarrow h \rightarrow \gamma\gamma$

Finally, we calculate the signal strength of the process  $gg \rightarrow h \rightarrow \gamma\gamma$  in our model. The bulk colored fermions contribute to both the effective Higgs coupling to digulon and diphoton, and hence alter this signal strength from the SM prediction. The signal strength is calculated by

$$\mu^{\gamma\gamma} \simeq \frac{\sigma(gg \rightarrow h \rightarrow \gamma\gamma)}{\sigma(gg \rightarrow h \rightarrow \gamma\gamma)_{\text{SM}}} = R_{gg} \times R_{\gamma\gamma}. \quad (6.21)$$



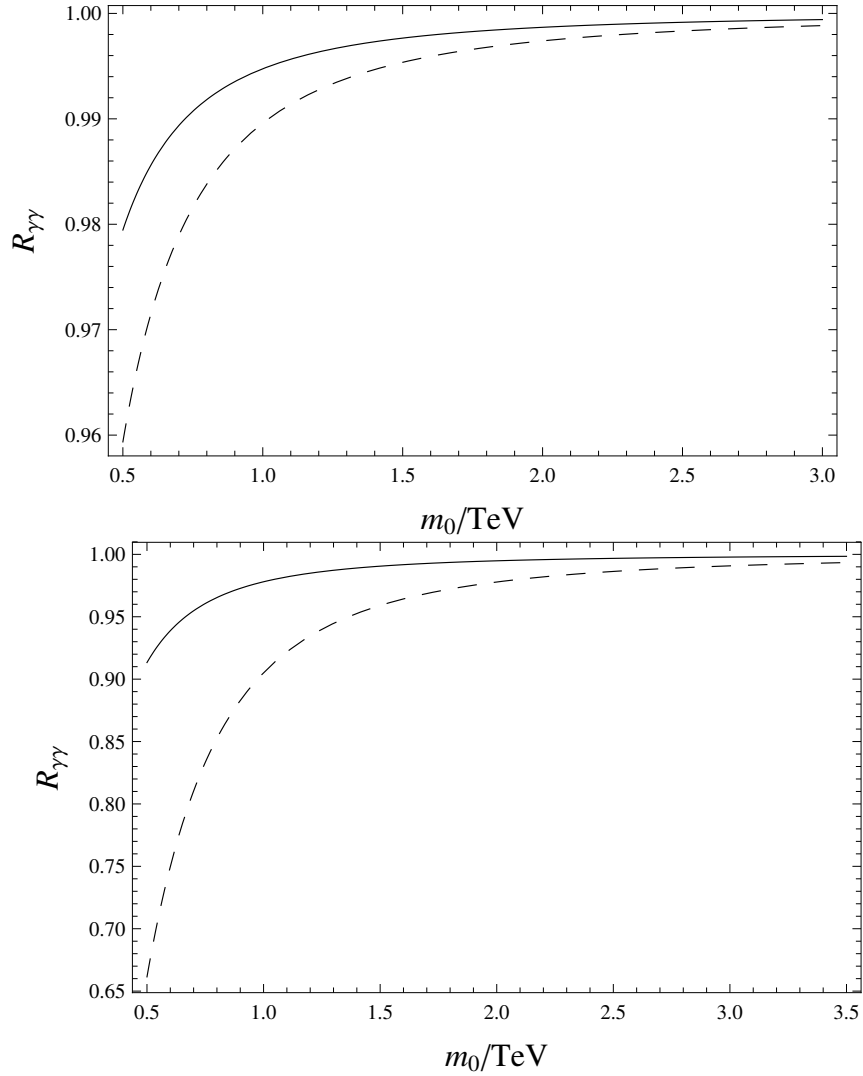


Fig. 6.2.: The signal strength for the Higgs diphoton decay mode in our model as a function of the lightest bulk fermion mass  $m_0$ . The top panel shows the results for the **6**-plet case corresponding to the top panel of Fig. 5.3. The results for the **10**-plet case, which correspond to the solid and dashed lines in Fig. 5.5, are depicted in the bottom panel.

We show our results in Fig. 6.3 for the color-triplet, **6**-plet (top panel) and **10**-plet fermions. The top panel shows the results for the **6**-plet case presented in the bottom panel of Fig. 5.3. The solid and dashed lines are corresponding to the same types of lines in the top panel of Fig. 5.3. The results for the **10**-plet case, which correspond to the dotted and the dash-dotted lines in Fig. 5.5, are depicted in the bottom panel. As the same in Fig. 6.1 the dotted line represents the case with the periodic boundary condition, while the dash-dotted line corresponds to the case with the half-periodic boundary condition. Employing the constraint,  $0.98 \leq \mu^{\gamma\gamma} \leq 1.36$ , from the ATLAS and CMS combined analysis [5], we can find a lower bound on  $m_0$  from Fig. 6.3. No lower bound can be obtained from the results on the top panel. For the **6**-plet fermions, we may apply the lower bound presented in Table 6.1. When we assign  $Q = 4/3$  to the **6**-plet fermions, the lightest mode has the color-triplet with an electric charge  $2/3$ , so that it can generally mix with the SM top quark. Through this mixing, once produced dominantly through the gluon fusion process at the LHC, it can decay into the  $W$ -boson/ $Z$ -boson/Higgs boson and top/bottom quark through the charged/neutral current. The current search for such a vector-like color triplet particle at the LHC has set lower mass limits between 720 and 920 GeV at 95% confidence level [39], which are more severe than those listed in Table 6.1. The lower bounds on  $m_0$  can be read off from the bottom panel in Fig. 6.3 and are summarized in Table 6.3. Comparing Tables 6.1 and 6.3, we see that the lower mass bounds from  $\mu^{\gamma\gamma}$  for the **10**-plet are more severe than those from  $R_{gg}$  and the direct search at the LHC.

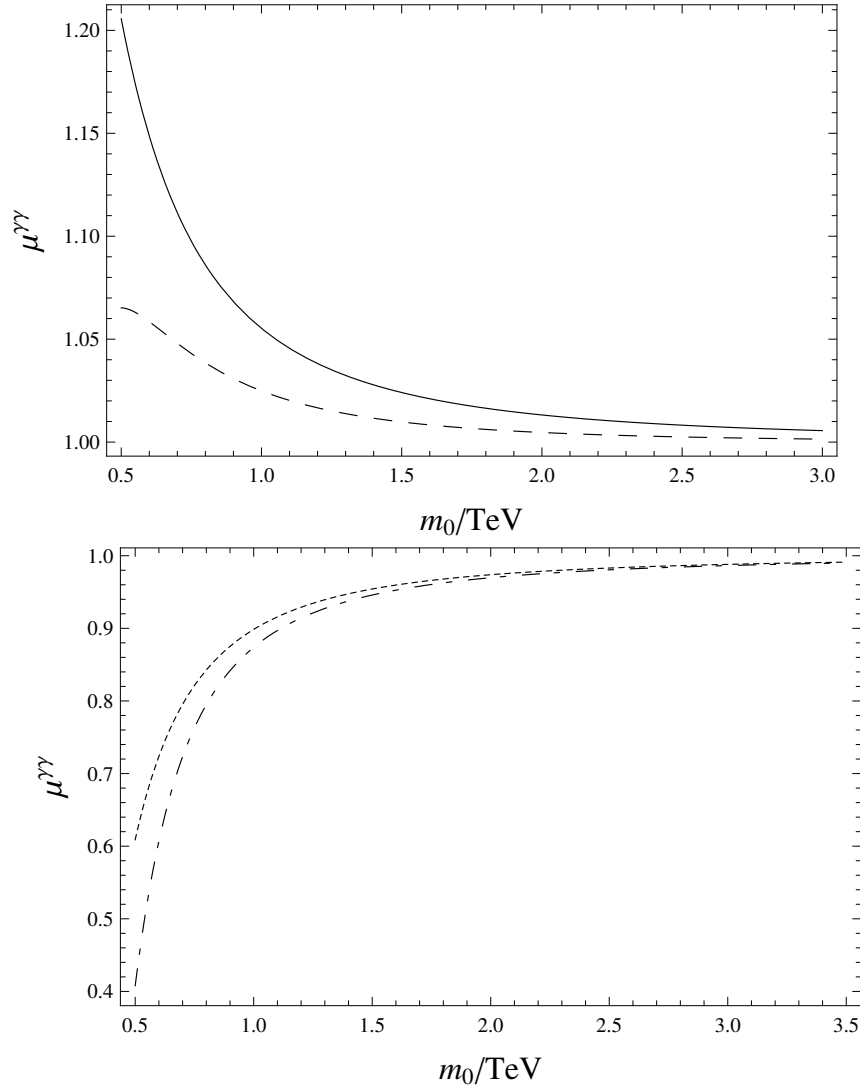


Fig. 6.3.: The signal strength as a function of the lightest bulk fermion mass  $m_0$ . The top panel shows the results for the **6**-plet case corresponding to the top panel of Fig. 5.3. The results for the **10**-plet case, corresponding to the dotted and dash-dotted lines in Fig. 5.5, are depicted in the bottom panel. Here we have considered the periodic boundary condition for the dotted line in Fig. 5.5, while the half-periodic boundary condition for the dash-dotted line Fig. 5.5. The dotted and dash-dotted lines represent the results for the periodic and half-periodic **10**-plet fermions, respectively.

## 7 CONCLUSIONS

Since the discovery of the SM Higgs boson at the LHC, the properties of the Higgs boson have been investigated towards the experimental confirmation of the origin of mass and electroweak symmetry breaking in the SM. The LHC Run II with the upgrade of the collider energy to 13 TeV is in operation and more data is being accumulated. In the near future, the Higgs boson properties such as its mass and decay rates to a variety of modes will be more accurately measured, by which the Higgs sector in the SM may be precisely confirmed or some deviation from the SM framework may be revealed.

The gauge hierarchy problem is one of the most serious problems of the SM, and many new physics models have been proposed towards a solution to the problem. Such new physics models include new particles whose couplings to the SM Higgs doublet influence the Higgs boson properties. For example, in the minimal supersymmetric standard model, there is a correlation between the Higgs boson mass and the mass of sparticles, in particular, scalar top quarks.

In this dissertation, we have considered the gauge-Higgs unification scenario in 5-dimensional flat space-time, where the SM Higgs doublet is embedded in the 5th spacial component of the gauge field in 5-dimensions. Thanks to the gauge symmetry, the quadratic divergence of the Higgs self-energy is forbidden and as a result, the gauge hierarchy problem can be solved. The gauge symmetry also forbids the Higgs potential at the tree-level, which is generated through quantum corrections with the breaking of the original bulk gauge symmetry down to the SM one. Thus, once the model is defined, the Higgs potential is in principle calculable and the Higgs boson mass can be predicted. However, it is highly non-trivial to offer a concrete GHU model which lead to not only a realistic Higgs potential but also all realistic SM fermion mass matrices.

In analyzing the Higgs boson properties in the context of the GHU scenario, there is a powerful approach in low energy effective theoretical point of view. Independently of details of the GHU models, the Higgs potential must disappear once the bulk gauge symmetry is

restored at some high energy, which is identified as the compactification scale by analysis of the effective Higgs potential in a simple GHU model. In low energy effective theory where all the KK modes are decoupled, this general feature of the GHU scenario yields the so-called gauge-Higgs condition, namely, the Higgs quartic coupling is set to be zero at the compactification scale. Therefore, under the assumption that the electroweak symmetry breaking is realized, the Higgs boson mass can be calculated by extrapolating the vanishing Higgs quartic coupling at the compactification scale towards low energies.

For a simple GHU model based on the bulk gauge group  $SU(3) \times U(1)'$ , we have analyzed the RG equations with the gauge-Higgs boundary condition to reproduce the observed Higgs boson pole mass of  $m_H = 125.09$  GeV. If we assume only the SM particle contents below the compactification scale, the Higgs boson mass is realized by  $M_{KK} \simeq 10^{10}$  GeV. We have introduced bulk fermions with a bulk mass and imposed a periodic or half-periodic boundary condition. For concreteness, we have considered color-singlet/triplet, **6** and **10**-plets of  $SU(3)$  with a  $U(1)'$  charge  $Q$ . Once the fermion representation is fixed, we have found a unique relation between the compactification scale and the bulk mass so as to reproduce  $m_H = 125.09$  GeV. We have found  $M_{KK} \ll 10^{10}$  GeV in the presence of the bulk fermions with the TeV scale mass.

We also have investigated the effect of the bulk fermions on the Higgs boson phenomenology. The bulk fermions contribute to the effective Higgs couplings to di-gluon and/or di-photon through quantum correction at the one-loop level, and as a result, the Higgs boson production and decay rates at the LHC can be altered from the SM predictions. We have employed the current LHC data, which are consistent with the SM predictions, and derived the lower mass bound on the lightest KK mode fermion. More precise measurements of the Higgs production and decay rates in the future can indirectly test the existence of the bulk fermions.

As pointed out in the second paper on Ref. [8], the bulk fermions, if their masses lie in the TeV scale, can also be tested directly at the LHC. A bulk fermion multiplet includes many fermions with a variety of electric charges, and the mass splittings among the fermions are predicted after the electroweak symmetry breaking. Hence, a heavy fermion, once produced at the LHC, causes cascade decays to lighter mass eigenstates and the weak gauge bosons or

the Higgs boson, which end up with the lightest KK mode fermion. The lightest KK mode fermion can be a dark matter candidate if it is stable, or decays to the SM fermion through a mixing between them. The existence of the variety of fermion mass eigenstates and their cascade decay at the LHC are characteristic feature of our GHU model. Search for the KK mode fermions at the LHC Run II is an interesting topic and we leave it for future work.

## REFERENCES

- [1] G. Degrandi, S. Di Vita, J. Elias-Miro, J. R. Espinosa, G. F. Giudice, G. Isidori, and A. Strumia, “Higgs mass and vacuum stability in the Standard Model at NNLO,” *JHEP* **08** (2012) 098, arXiv:1205.6497 [hep-ph].
- [2] **ATLAS** Collaboration, G. Aad *et al.*, “Observation of a new particle in the search for the Standard Model Higgs boson with the ATLAS detector at the LHC,” *Phys. Lett.* **B716** (2012) 1–29, arXiv:1207.7214 [hep-ex].
- [3] **CMS** Collaboration, S. Chatrchyan *et al.*, “Observation of a new boson at a mass of 125 GeV with the CMS experiment at the LHC,” *Phys. Lett.* **B716** (2012) 30–61, arXiv:1207.7235 [hep-ex].
- [4] **ATLAS, CMS** Collaboration, G. Aad *et al.*, “Combined Measurement of the Higgs Boson Mass in  $pp$  Collisions at  $\sqrt{s} = 7$  and 8 TeV with the ATLAS and CMS Experiments,” *Phys. Rev. Lett.* **114** (2015) 191803, arXiv:1503.07589 [hep-ex].
- [5] **CMS** Collaboration, C. Collaboration, “Measurements of the Higgs boson production and decay rates and constraints on its couplings from a combined ATLAS and CMS analysis of the LHC  $pp$  collision data at  $\sqrt{s} = 7$  and 8 TeV,”.
- [6] H. Hatanaka, T. Inami, and C. S. Lim, “The Gauge hierarchy problem and higher dimensional gauge theories,” *Mod. Phys. Lett.* **A13** (1998) 2601–2612, arXiv:hep-th/9805067 [hep-th].
- [7] N. Haba, S. Matsumoto, N. Okada, and T. Yamashita, “Effective theoretical approach of Gauge-Higgs unification model and its phenomenological applications,” *JHEP* **02** (2006) 073, arXiv:hep-ph/0511046 [hep-ph].
- [8] N. Maru and N. Okada, “Diphoton decay excess and 125 GeV Higgs boson in gauge-Higgs unification,” *Phys. Rev.* **D87** no. 9, (2013) 095019, arXiv:1303.5810 [hep-ph].
- [9] N. Maru and N. Okada, “125 GeV Higgs Boson and TeV Scale Colored Fermions in Gauge-Higgs Unification,” arXiv:1310.3348 [hep-ph].
- [10] C. P. Burgess and G. D. Moore, *The standard model: A primer*. Cambridge University Press, 2006.
- [11] M. Srednicki, *Quantum field theory*. Cambridge University Press, 2007.

- [12] M. E. Peskin and D. V. Schroeder, *An Introduction to quantum field theory*. 1995.  
<http://www.slac.stanford.edu/spires/find/books/www?cl=QC174.45>
- [13] P. W. Higgs, “Broken symmetries, massless particles and gauge fields,” *Phys. Lett.* **12** (1964) 132–133.
- [14] P. W. Higgs, “Broken Symmetries and the Masses of Gauge Bosons,” *Phys. Rev. Lett.* **13** (1964) 508–509.
- [15] A. de Gouvea, D. Hernandez, and T. M. Tait, “Criteria for Natural Hierarchies,” *Phys. Rev.* **D89** no. 11, (2014) 115005, [arXiv:1402.2658](https://arxiv.org/abs/1402.2658) [hep-ph].
- [16] J. Elias-Miro, J. R. Espinosa, G. F. Giudice, G. Isidori, A. Riotto, and A. Strumia, “Higgs mass implications on the stability of the electroweak vacuum,” *Phys. Lett.* **B709** (2012) 222–228, [arXiv:1112.3022](https://arxiv.org/abs/1112.3022) [hep-ph].
- [17] S. P. Martin, “A Supersymmetry primer,” [arXiv:hep-ph/9709356](https://arxiv.org/abs/hep-ph/9709356) [hep-ph]. [Adv. Ser. Direct. High Energy Phys.18,1(1998)].
- [18] N. Arkani-Hamed, S. Dimopoulos, and G. Dvali, “The Hierarchy problem and new dimensions at a millimeter,” *Phys. Lett.* **B429** (1998) 263–272, [arXiv:hep-ph/9803315](https://arxiv.org/abs/hep-ph/9803315) [hep-ph].
- [19] L. Randall and R. Sundrum, “A Large mass hierarchy from a small extra dimension,” *Phys. Rev. Lett.* **83** (1999) 3370–3373, [arXiv:hep-ph/9905221](https://arxiv.org/abs/hep-ph/9905221) [hep-ph].
- [20] G. Cacciapaglia, C. Csaki, and S. C. Park, “Fully radiative electroweak symmetry breaking,” *JHEP* **03** (2006) 099, [arXiv:hep-ph/0510366](https://arxiv.org/abs/hep-ph/0510366) [hep-ph].
- [21] N. Maru and N. Okada, “Gauge-Higgs unification at LHC,” *Phys. Rev.* **D77** (2008) 055010, [arXiv:0711.2589](https://arxiv.org/abs/0711.2589) [hep-ph].
- [22] C. A. Scrucca, M. Serone, and L. Silvestrini, “Electroweak symmetry breaking and fermion masses from extra dimensions,” *Nucl. Phys.* **B669** (2003) 128–158, [arXiv:hep-ph/0304220](https://arxiv.org/abs/hep-ph/0304220) [hep-ph].
- [23] N. Arkani-Hamed and M. Schmaltz, “Hierarchies without symmetries from extra dimensions,” *Phys. Rev.* **D61** (2000) 033005, [arXiv:hep-ph/9903417](https://arxiv.org/abs/hep-ph/9903417) [hep-ph].
- [24] G. Martinelli, M. Salvatori, C. A. Scrucca, and L. Silvestrini, “Minimal gauge-Higgs unification with a flavour symmetry,” *JHEP* **10** (2005) 037, [arXiv:hep-ph/0503179](https://arxiv.org/abs/hep-ph/0503179) [hep-ph].
- [25] B. He, N. Okada, and Q. Shafi, “Higgs Boson Mass Bounds in Seesaw Extended Standard Model with Non-Minimal Gravitational Coupling,” *Phys. Lett.* **B695** (2011) 219–224, [arXiv:1009.1878](https://arxiv.org/abs/1009.1878) [hep-ph].



- [26] G. von Gersdorff, N. Irges, and M. Quiros, “Finite mass corrections in orbifold gauge theories,” 2002. [arXiv:hep-ph/0206029](#) [hep-ph].
- [27] I. Gogoladze, N. Okada, and Q. Shafi, “Higgs boson mass from gauge-Higgs unification,” *Phys. Lett.* **B655** (2007) 257–260, [arXiv:0705.3035](#) [hep-ph].
- [28] S. R. Coleman and E. J. Weinberg, “Radiative Corrections as the Origin of Spontaneous Symmetry Breaking,” *Phys. Rev.* **D7** (1973) 1888–1910.
- [29] M. Sher, “Electroweak Higgs Potentials and Vacuum Stability,” *Phys. Rept.* **179** (1989) 273–418.
- [30] D. Buttazzo, G. Degrassi, P. P. Giardino, G. F. Giudice, F. Sala, A. Salvio, and A. Strumia, “Investigating the near-criticality of the Higgs boson,” *JHEP* **12** (2013) 089, [arXiv:1307.3536](#) [hep-ph].
- [31] **ATLAS, CDF, CMS, D0** Collaboration, “First combination of Tevatron and LHC measurements of the top-quark mass,” [arXiv:1403.4427](#) [hep-ex].
- [32] N. Haba, S. Matsumoto, N. Okada, and T. Yamashita, “Gauge-Higgs Dark Matter,” *JHEP* **03** (2010) 064, [arXiv:0910.3741](#) [hep-ph].
- [33] M. Regis, M. Serone, and P. Ullio, “A Dark Matter Candidate from an Extra (Non-Universal) Dimension,” *JHEP* **03** (2007) 084, [arXiv:hep-ph/0612286](#) [hep-ph].
- [34] G. Panico, E. Ponton, J. Santiago, and M. Serone, “Dark Matter and Electroweak Symmetry Breaking in Models with Warped Extra Dimensions,” *Phys. Rev.* **D77** (2008) 115012, [arXiv:0801.1645](#) [hep-ph].
- [35] M. Carena, A. D. Medina, N. R. Shah, and C. E. M. Wagner, “Gauge-Higgs Unification, Neutrino Masses and Dark Matter in Warped Extra Dimensions,” *Phys. Rev.* **D79** (2009) 096010, [arXiv:0901.0609](#) [hep-ph].
- [36] Y. Hosotani, P. Ko, and M. Tanaka, “Stable Higgs Bosons as Cold Dark Matter,” *Phys. Lett.* **B680** (2009) 179–183, [arXiv:0908.0212](#) [hep-ph].
- [37] D. Buttazzo, G. Degrassi, P. P. Giardino, G. F. Giudice, F. Sala, A. Salvio, and A. Strumia, “Investigating the near-criticality of the Higgs boson,” *JHEP* **12** (2013) 089, [arXiv:1307.3536](#) [hep-ph].
- [38] J. R. Ellis, M. K. Gaillard, and D. V. Nanopoulos, “A Phenomenological Profile of the Higgs Boson,” *Nucl. Phys.* **B106** (1976) 292.
- [39] **CMS** Collaboration, V. Khachatryan *et al.*, “Search for vector-like charge 2/3 T quarks in proton-proton collisions at  $\sqrt{s} = 8$  TeV,” [arXiv:1509.04177](#) [hep-ex].